BJ www.biochemj.org

BJ Metabolism

Biochem. J. (2010) **425**, 71–83 (Printed in Great Britain) doi:10.1042/BJ20090928

online data

Brd2 disruption in mice causes severe obesity without Type 2 diabetes

Fangnian WANG*, Hongsheng LIU*, Wanda P. BLANTON*†‡, Anna BELKINA*, Nathan K. LEBRASSEUR§[1] and Gerald V. DENIS*†[2]

*Cancer Research Center, Boston University School of Medicine, Boston, MA 02118, U.S.A., †Immunology Training Program, Boston University School of Medicine, Boston, MA 02118, U.S.A., ‡Section of Gastroenterology, Boston University School of Medicine, Boston, MA 02118, U.S.A., and §Section of Endocrinology, Diabetes and Nutrition, Boston University School of Medicine, Boston, MA 02118, U.S.A.

Certain human subpopulations are metabolically healthy but obese, or metabolically obese but normal weight; such mutations uncouple obesity from glucose intolerance, revealing pathways implicated in Type 2 diabetes. Current searches for relevant genes consume significant effort. We have reported previously a novel double bromodomain protein called Brd2, which is a transcriptional co-activator/co-repressor with SWI/SNF (switch mating type/sucrose non-fermenting)-like functions that regulates chromatin. In the present study, we show that whole-body disruption of *Brd2*, an unusual MHC gene, causes lifelong severe obesity in mice with pancreatic islet expansion, hyperinsulinaemia, hepatosteatosis and elevated pro-inflammatory cytokines, but, surprisingly, enhanced glucose tolerance, elevated adiponectin, increased weight of brown adipose tissue, heat production and expression of mitochondrial uncoupling proteins in brown adipose tissue, reduced macrophage infiltration in white adipose tissue, and lowered blood glucose, leading to an improved metabolic profile and avoiding eventual Type 2 diabetes. Brd2 is highly expressed in pancreatic β-cells, where it normally inhibits β-cell mitosis and insulin transcription. In 3T3-L1 pre-adipocytes, Brd2 normally co-represses PPAR-γ (peroxisome-proliferator-activated receptor-γ) and inhibits adipogenesis. Brd2 knockdown protects 3T3-L1 adipocytes from TNF-α (tumour necrosis factor-α)-induced insulin resistance, thereby decoupling inflammation from insulin resistance. Thus hypomorphic Brd2 shifts energy balance toward storage without causing glucose intolerance and may provide a novel model for obese metabolically healthy humans.

Key words: adipogenesis, β-cell, Brd2, bromodomain, energy balance, obesity, Type 2 diabetes.

INTRODUCTION

The problem of human obesity worldwide has reached a crisis in scope and is expected to result in dramatic increases in obesity-related morbidity and early mortality [1]. Much of the projected global incidence of 366 million diabetic individuals by 2030 is expected to be obesity-driven [2]. Thus a deeper molecular understanding of the origins of diabetes is urgently required, particularly signal transduction systems that couple obesity to Type 2 diabetes. Recently, attention has focused on human subpopulations that appear to harbour mutations that uncouple obesity from insulin resistance, because of the opportunity they provide to increase our understanding of the aetiology of obesity-driven diabetes; the molecular mechanisms that drive these processes remain incompletely understood. Such individuals may be either MHO (metabolically healthy but obese) or MONW (metabolically obese but normal weight) [3]. Evidence we provide in the present study suggests that a recently described double bromodomain protein called Brd2 is functionally required *in vivo* to couple obesity to eventual Type 2 diabetes.

Brd2, formerly 'RING3', was first identified as a close homologue of TAF (TATA-box-binding protein-associated factor)$_{II}$250, a basal transcription co-activator [4]. The gene resides on human chromosome 6p within the MHC class II locus and is found in syntenic regions of other organisms [5]. In mammals, the MHC class II genes encode molecules that participate in processing and presentation of antigenic peptides to T-cells, except *BRD2*, which encodes a double bromodomain protein that shares no significant sequence similarity to or function with other MHC class II molecules and has been suggested to be involved in signal transduction [6]. Brd2 is one of the protein factors that regulate gene transcription by controlling the activity of transcription complexes, interpreting the histone code and remodelling chromatin. Brd2 belongs to the BET (bromodomain and extraterminal domain) subfamily of proteins that harbour two bromodomains [7]. The bromodomain is a conserved protein motif comprised of approx. 110 amino acids that form four α-helices connected by two loops; the motif binds acetyl-lysine residues of nucleosomal histones [8]. Bromodomain proteins serve as adaptor or scaffolding modules that recruit transcription regulatory factors to chromatin to form protein complexes that regulate gene transcription in response to signal transduction [9,10]. Bromodomains are found in the DNA helicase superfamily members [11] brahma/Brm/Snf2α or Brg1/Snf2β, which are the core catalytic ATPase subunits of the SWI/SNF (switch mating type/sucrose non-fermenting) nucleosome remodelling complex [12]. The bromodomain structure itself does not possess Hat (histone acetyltransferase) activity or other catalytic functions, but

Abbreviations used: ACC, acetyl-CoA carboxylase; BAT, brown adipose tissue; BET, bromodomain and extraterminal domain; BrdU, bromodeoxyuridine; ES, embryonic stem; *fsh*, *female sterile (1) homeotic*; Hat, histone acetyltransferase; Hdac, histone deacetylase; HFD, high-fat diet; IGTT, intraperitoneal glucose tolerance test; IL-1β, interleukin-1β; MHO, metabolically healthy but obese; MONW, metabolically obese but normal weight; NCBI, National Center for Biotechnology Information; NEFA, non-esterified fatty acid ('free fatty acid'); PPAR-γ, peroxisome-proliferator-activated receptor-γ; PGC, PPAR-γ co-activator; Pten, phosphatase and tensin homologue deleted on chromosome 10; RER, respiratory exchange ratio; RT, reverse transcription; shRNA, small-hairpin RNA; SVF, stromal vascular fraction; SWI/SNF, switch mating type/sucrose non-fermenting; TAF, TATA-box-binding protein-associated factor; TNF-α, tumour necrosis factor-α; Ucp, uncoupling protein.

[1] Present address: Cardiovascular, Metabolic and Endocrine Diseases, Pfizer Global Research and Development, Groton, CT 06340, U.S.A.

[2] To whom correspondence should be addressed (email gdenis@bu.edu).

it is found in many transcriptional and developmental regulators that function through histone modification and nucleosome remodelling [7–10].

Brd2 is a signal transducer [13] and a nuclear-localized serine/threonine kinase [13,14], and is ubiquitously expressed in mammalian tissues [15]. Brd2 binds to ε-aminoacetyl groups of nucleosomal histone lysine residues with its two bromodomains, particularly acetyl-histone H4 [16], and participates in multiprotein transcription complexes such as Mediator [17]. We have shown previously that Brd2 binds not only transcriptional activators like E2F proteins, but also co-activator TAFs, members of the SWI/SNF complex, Hats and Hdacs (histone deacetylases) [18] to regulate the expression of diverse genes [19]. As with the SWI/SNF complex with which it associates, Brd2 can function as either a transcriptional co-activator or co-repressor, depending on the specific promoter and cellular context [20,21].

One or the other of the Brd2 yeast homologues *BDF1* and *BDF2* are essential for yeast viability; double mutants are lethal [22]. Bdf1 and yTaf145 together serve a functional role similar to $TAF_{II}250$ in mammals [23]. Bdf1 has been suggested to play a role in chromatin restructuring [24]. The *Drosophila* homologue [4,25] of *Brd2*, *fsh* [*female sterile (1) homeotic*] is a maternal effect gene that encodes a double bromodomain-containing developmental factor that restructures chromatin as a co-activator or co-repressor. During *Drosophila* development, *fsh* acts as an upstream activator of Hox genes such as *trithorax* [26] and the *Ultrabithorax* complex [25], which counter Polycomb repression. Mutation of *fsh* causes severe homoeotic defects that resemble *trithorax* mutations [26] and homozygous mutation is lethal [27].

To study Brd2 function *in vivo*, we expressed it constitutively in the B-cells of transgenic mice, where it causes B-cell lymphoma and leukaemia [28]. A related protein, called Brd4, is also a chromatin regulator and transcriptional adapter [29]. Brd4 binds acetylated histones [30] and is necessary for the G_2-to-M transition of the cell cycle [31]. As with *fsh*-deficient flies, $brd4^{(+/-)}$ mice have severe developmental defects; $brd4^{(-/-)}$ is lethal [32]. Our next step in the characterization of the *in vivo* function of Brd2 was to engineer a knockout mouse. Given the above considerations, we expected $brd2^{(-/-)}$ to be lethal in mice. Consistent with this expectation, we could not obtain $brd2^{(-/-)}$-null mice or ES (embryonic stem) cells, and in support of this result, recent reports have established that *Brd2* is essential because $brd2^{(-/-)}$-null mice have neural tube defects and embryonic lethality [33,34]. However, we found, surprisingly, that targeted disruption of the *Brd2* gene in the promoter region, leading to the reduced expression of Brd2 ('*brd2 lo*'; *w/lo*), produces a hypomorphic phenotype without gross developmental abnormalities. These mice have extreme obesity with hyperinsulinaemia, but enhanced glucose tolerance and low blood glucose, which is quite distinct from other animal models of obesity.

EXPERIMENTAL

ES cell lines and mice

RRT234 and RRE050 murine ES cell lines were purchased from BayGenomics and were used for microinjection. Homozygous $brd2^{(-/-)}$ ES cells (234/DK; see Figure 1D) were derived from the RRT234 parental line by culturing cells in medium with 8 mg/ml G418. C57BL/6J mice were from the Jackson Laboratory. The regular chow (2918 formulation; Harlan Teklad) was irradiated and contained 57.3 % carbohydrate. Animals were handled humanely in accordance with Boston University IACUC, State and Federal regulatory requirements. Please refer to the Supplementary Experimental section available at http://www.BiochemJ.org/bj/425/bj4250071add.htm for additional details.

Metabolic measurements

$\dot{V}_{O_2}$ (oxygen consumption) and $\dot{V}_{CO_2}$ (carbon dioxide production) were measured by indirect calorimetry and was used to calculate RER (respiratory exchange ratio) and heat production (CLAMS; Columbus Instruments). Glucose was determined in fresh whole-blood samples using a Glucometer Elite (Bayer). Plasma hormone, cytokine and lipid measurements were performed at the Specialized Assay Core, Joslin Diabetes Center, Boston, MA, U.S.A.

Immunohistochemistry

Brd2 protein was detected with a rabbit polyclonal antibody as described previously [14].

Flow cytometry

Unless otherwise indicated, all reagents were from eBioscience. Standard flow protocols were used and are described in detail in the Supplementary Experimental section.

3T3-L1 pre-adipocyte differentiation and assays

Standard differentiation protocols were used and are described in detail in the Supplementary Experimental section.

Protein immunoblotting and co-immunoprecipitation

Immunoblotting and co-immunoprecipitation were performed according to the manufacturer's instructions (Santa Cruz Biotechnology) and as described previously [14].

Luciferase assay

Briefly, 3T3-L1 pre-adipocytes were transfected in 24-well plates using Lipofectamine™ 2000 (Invitrogen). Transfections typically consisted of 0.1 μg of tk-PPRE3X-luc (Addgene), 0.015 μg of pRL (Promega), 0.18 μg of pFlag.PPAR-γ (Addgene) and 0.5 μg of effector (pSiBrd2, pmBrd2 or control vectors). Cell lysates were harvested 48 h after transfection and luciferase activity was measured using a Dual Luciferase Reporter Assay System (Promega) on a TD-20/20 luminometer (Turner Biosystems).

Statistical analysis

Values are shown as means $\pm$ S.E.M. Paired Student's *t* tests were used to compare means, and $P < 0.05$ was considered significant. Details on the analyses used are described in the Supplementary Experimental section.

RESULTS

Generation and phenotype of *w/lo* mice

We attempted to generate *Brd2*-knockout mice using two *Brd2* gene-trapped murine ES cell lines from BayGenomics (RRE050 and RRT234). Gene trap vectors were inserted into intron 1, 5′ to the first ATG codon of the *Brd2* gene in RRT234 cells, or into intron 2, 3′ to the first ATG codon in RRE050

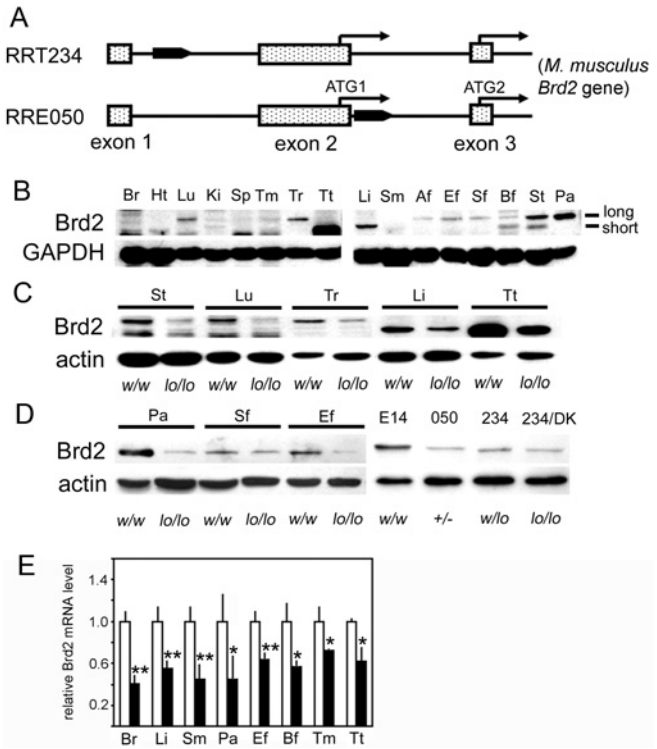

Figure 1 Engineering of obese *w*/*lo* mice

(**A**) *Brd2* gene trap events in RRT234 and RRE050 ES cell lines. The filled pointed rectangular box indicates the gene trap vector. (**B**) Brd2 expression in *w*/*w* mice detected by immunoblotting with a Brd2 antibody. GAPDH, glyceraldehyde-3-phosphate dehydrogenase. (**C**) Brd2 protein expression in genetically engineered mice. (**D**) Brd2 protein expression in tissues and ES cell lines. E14, parental E14Tg2A ES cell line; 050, RRE 050 ES cell line; 234, RRT234 ES cell line; 234/DK, *brd2* double-mutant RRT234 ES cell line; +/−, heterozygous *brd2* knockout from RRE050 ES cells. (**E**) Quantitative real-time PCR analysis of *Brd2* mRNA expression in tissues from heterozygous *w*/*lo* mice from RRT234 ES cells (closed bars) and control *w*/*w* male mice (open bars) age-matched at 6 months ($n = 3$; $^{*}P < 0.05$ and $^{**}P < 0.01$). Af, abdominal fat; Bf, BAT; Br, brain; Ef, epididymal fat pad; Ht, heart; Ki, kidney; Lu, lung; Li, liver; Pa, pancreas; Sf, subcutaneous fat; Sm, skeletal muscle; Sp, spleen; St, stomach; Tm, thymus; Tr, thyroid; Tt, testis.

cells (Figure 1A). The RRE050 disruption (the ES cells used by Shang et al. [33]) reduced Brd2 expression levels more drastically than did the RRT234 disruption (Figures 1C and 1D). Germline transfer succeeded with blastocyst microinjection of RRT234, but not with RRE050, suggesting that Brd2 is critical for embryogenesis, similar to Brd4 [32]. Male chimaeras from RRT234 microinjection were crossed with C57BL/6J female mice to produce heterozygous (F1) *Brd2*-mutant animals on a 129P2 and C57BL/6J mixed background. The male F1 heterozygote mice were then back-crossed to female wild-type C57BL/6J mice for five generations (F5), then the F5 male and female heterozygotes were mated to produce wild-type (*w*/*w*), heterozygous (*w*/*lo*; '*brd2 lo*') and homozygous (*lo*/*lo*) animals for study.

To determine whether gene trap insertion into the first intron of *Brd2* in RRT234 ES cells disrupts Brd2 expression *in vivo* and *in vitro*, first we measured Brd2 protein expression in different tissues of *w*/*w* mice. There are at least two forms of Brd2 protein in mice due to alternative mRNA splicing and/or alternative start codons for translation. The long form is comprised of 798 amino acids [NCBI (National Center for Biotechnology Information) accession number NP_034368] and the short form of 679 amino acids (NCBI accession number NP_001020558). Immunoblot analysis showed that, in adult *w*/*w* mice, the long form is mainly expressed in lung, thyroid, stomach and pancreas, with low expression in adipose tissues. The short form is mainly expressed in testis, liver, BAT (brown adipose tissue) and stomach (Figure 1B). Unexpectedly, the RRT234 mutation reduced rather than eliminated the expression of both forms of Brd2, as shown by immunoblot analysis of Brd2 for all of the tested tissues from homozygous mice (*lo*/*lo*; Figures 1C and 1D) and a homozygous RRT234 ES cell line (double knockout; Figure 1D). Heterozygous mice also had reduced expression (Figure 1E). Live births of homozygous mice were extremely rare and did not yield sufficient animals for study (see Supplementary Table S1 available at http://www.BiochemJ.org/bj/425/bj4250071add.htm). Thus, with RRT234 ES cells, we generated a Brd2 hypomorph (*w*/*lo*; '*brd2 lo*') mouse line.

The *w*/*lo* mice were viable and appeared normal at birth, but, surprisingly, they gradually became extremely obese on a diet of regular chow *ad libitum* (Figure 2A). The penetrance of this phenotype was 100 %. Body weights of *w*/*lo* mice diverged from control mice at around 2 months of age, reached 60 g by 4 months of age and continually increased to 90 g by 14 months of age (Figure 2B). Interestingly, the difference in body weight between *w*/*lo* mice and *w*/*w* mice held steady at 40–50 g at 4 months and thereafter, suggesting a higher 'set point' for the body weight of *w*/*lo* mice. Body fat deposition was abundant and widespread. Epididymal fat pads were three times heavier than *w*/*w* controls of the same age [1.57 ± 0.16 g in *w*/*w* mice compared with 6.32 ± 0.50 g in *w*/*lo* mice ($n = 3$; $P < 0.01$)]. Most dramatically, skeletal muscle was encased in thick layers of fat with adipose deposits throughout. Histopathologically, obese *w*/*lo* mice shared certain features with other obese mouse models. Small adipocytes ($\leqslant 2000\ \mu m^2$ in area) were present in equal numbers in epididymal fat pads of *w*/*w* mice and obese *w*/*lo* mice (Mann–Whitney rank sum, $P = 0.256$), but enlarged adipocytes ($>2000\ \mu m^2$) typified the fat depots of obese *w*/*lo* mice ($P < 0.001$); 1.1 % of *w*/*w* mice and 62.9 % of *w*/*lo* mice epididymal adipocytes were larger than $10000\ \mu m^2$, and 3.6 % of *w*/*w* mice and 48.1 % of *w*/*lo* mice subcutaneous adipocytes were larger than $10000\ \mu m^2$ (Figures 2C–2E), consistent with greatly increased storage in *w*/*lo* mice. The *w*/*w* mice and *w*/*lo* mice shared the same relationship between pancreatic islet area and β-cell number (Figure 2H); pancreatic islets were increased both in number and area in obese *w*/*lo* mice (Figures 2F and 2G) and some islets from *w*/*lo* mice were extremely large (Figures 2G and 2H). Increased islet number and size is consistent with other murine models of obesity, such as *ob*/*ob*, during development of insulin resistance and before the onset of Type 2 diabetes [35]. Islets of obese *w*/*lo* mice had high integrity (Figure 2F); β-cell failure, necrosis or declines in islet area or number were never observed in obese *w*/*lo* mice, at any age. Severe hepatosteatosis was also apparent in obese *w*/*lo* mice (Figure 2I).

Obesity is caused by increased energy storage and/or decreased energy expenditure. In general, obese animals are hyperphagic compared with wild-type; hyperphagia was also observed in obese *w*/*lo* mice. At 4 weeks of age, the *w*/*lo* mice had no statistically significant difference in food intake compared with *w*/*w* mice (3.9 ± 0.5 g in *w*/*w* mice compared with 4.0 ± 0.4 g in *w*/*lo* mice; $n = 3$), but at 8 weeks began to increase their food intake compared with *w*/*w* mice (Figure 3A), and they maintained this pattern as they aged. The obese *w*/*lo* mice were hyperinsulinaemic (Figure 3B), but, surprisingly, had low blood glucose (Figure 3C). We noticed the first signs of fed-state low blood glucose in *w*/*lo* mice as early as 4 weeks after birth (Figure 3C). Remarkably, fed-state glucose levels held near fasting-state thereafter (Figure 3C). To measure metabolic parameters, we housed obese *w*/*lo* mice and *w*/*w* mice individually in metabolic cages with regular chow *ad*

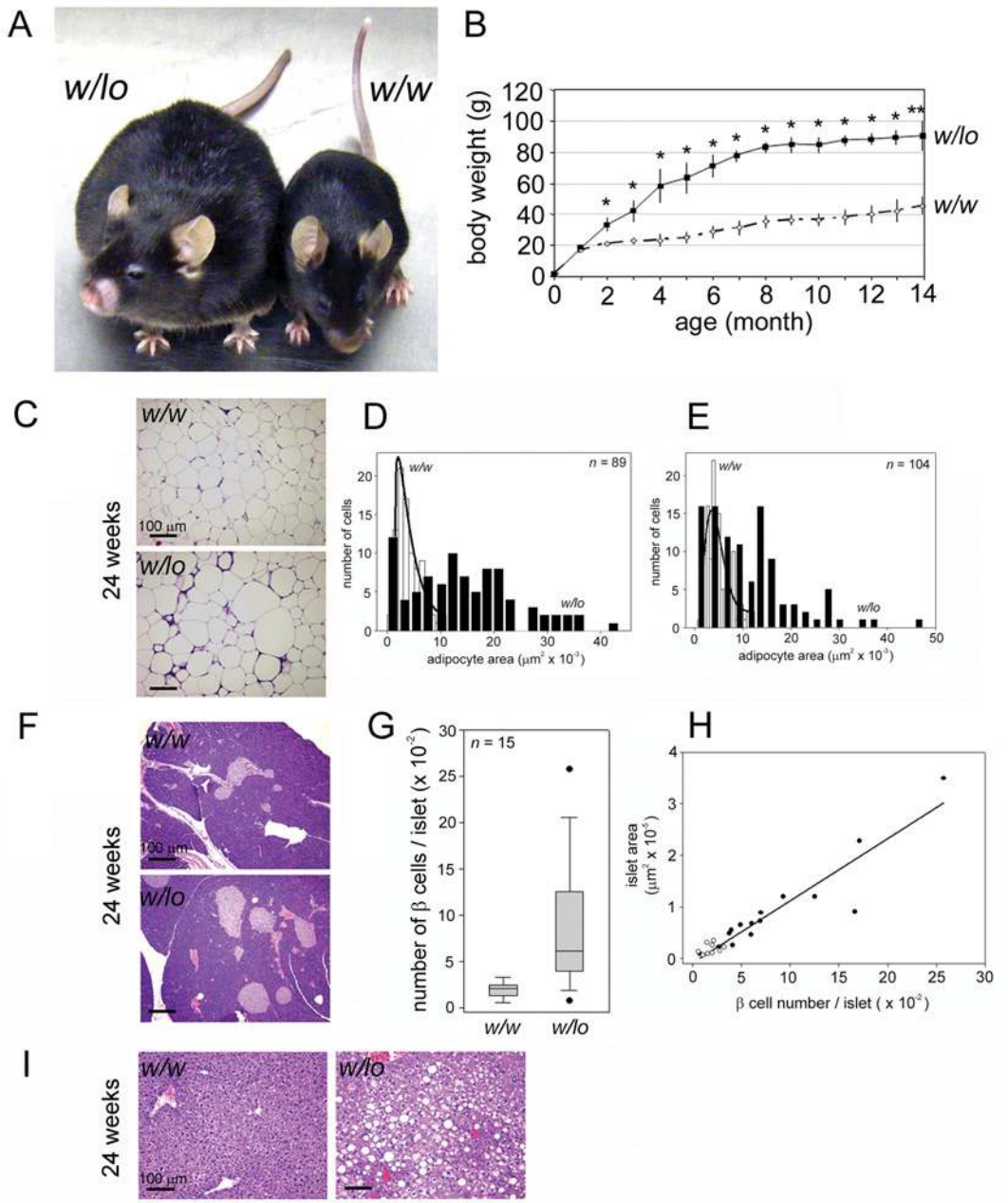

Figure 2 Whole-body reduction of Brd2 causes severe obesity in mice

(**A**) F6 generation of heterozygous *w*/*lo* and *w*/*w* control mice at 6 months of age. (**B**) Body weight curves of *w*/*lo* mice (◆) and *w*/*w* mice (◇) over time ($n = 4$–6; $^{*}P<0.05$ and $^{**}P<0.01$). (**C**) Histopathological changes in the epididymal fat pad of obese *w*/*lo* mice and *w*/*w* mice at 6 months of age. Image analysis of epididymal (**D**) and subcutaneous (**E**) adipocytes. Distribution curve fit by non-linear regression. *w*/*w* mice, open bars; *w*/*lo* mice, closed bars. (**F**) Histopathological changes in the pancreas of obese *w*/*lo* mice and *w*/*w* mice at 6 months of age. (**G**) Box plot analysis of β-cell number per islet from the pancreas of *w*/*w* mice and *w*/*lo* mice. (**H**) Regression of β-cell number/islet against islet area of the pancreas from *w*/*w* mice (○) and *w*/*lo* mice (●). (**I**) Histopathological changes in the liver of obese *w*/*lo* mice and *w*/*w* mice at 6 months of age. Sections were visualized with haematoxylin and eosin stain. Scale bar, 100 μm.

libitum and measured food intake, heat production by calorimetry and RER. Photocells aligned with the *x*-, *y*- and *z*- axes of the cages established that habitual activity was not significantly different from *w*/*w* mice (results not shown). The *w*/*lo* mice produced approximately twice as much heat than controls (Figure 3D). In further support of these data, obese *w*/*lo* mice carry twice as much interscapular BAT (257 ± 14 mg) as *w*/*w* mice (129 ± 52 mg) or *w*/*w* mice rendered obese by 4 months on a HFD (high-fat diet) (138 ± 20 mg) (Figure 3E), and had significant transcriptional up-regulation of Ucps 1, 2 and 3 (uncoupling proteins 1, 2 and 3) in BAT (Figure 3F). Strikingly, RER values of obese *w*/*lo* mice held at a fasting level regardless of actual feeding state (Figure 3G), suggesting they constantly catabolize fat stores as their major energy source. Thus *w*/*lo* obesity is not explained by reduced energy expenditure, but is more likely to be attributable to increased energy consumption and storage.

Obesity is a chronic disease and is usually accompanied by serological features such as hyperinsulinaemia, hyperleptinaemia, hypoadiponectinaemia, dyslipidaemia and elevated pro-inflammatory cytokines. Certain serological parameters of

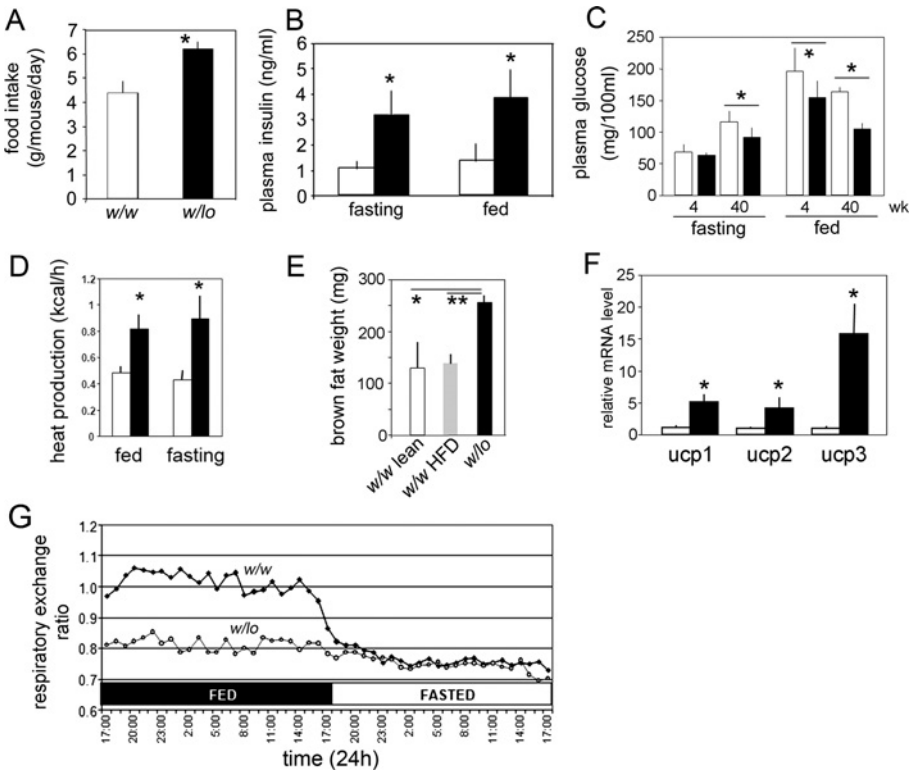

Figure 3 Metabolic changes in *w/lo* mice

(**A**) Hyperphagia of *w/lo* mice at 8 weeks compared with *w/w* mice at the same age ($n = 6$; $^*P = 0.0003$). (**B**) Hyperinsulinaemia in *w/lo* mice at 40 weeks (closed bars) compared with *w/w* mice at the same age (open bars) ($n = 4$; $^*P < 0.05$). (**C**) Obese *w/lo* mice develop fed-state low blood glucose as they age. Plasma glucose at 4 and 40 weeks of age for *w/lo* mice (closed bars) and *w/w* mice (open bars) ($n = 6$; $^*P < 0.05$). (**D**) Heat production at 40 weeks of age for obese *w/lo* mice (closed bars) and *w/w* mice (open bars) ($n = 4$; $^*P < 0.05$). (**E**) Weight of interscapular BAT depots of age-matched *w/w* and lean mice (*w/w* lean), *w/w* and obese mice after 4 months on an HFD (*w/w* HFD) or obese *w/lo* mice ($n = 3$; $^*P = 0.015$ and $^{**}P = 0.0017$). (**F**) Real-time RT–PCR assay of mRNA levels of Ucp1, 2 and 3 compared with β-actin in interscapular BAT from (**E**); (open bars) obese *w/w* mice; (closed bars) obese *w/lo* mice ($n = 3$; $^*P < 0.05$). (**G**) A representative RER of *w/w* mice (◆) and obese *w/lo* mice (◇) in fed and fasted states at 40 weeks.

the obese *w/lo* mice reflected chronic obesity. Plasma levels of hormones, such as insulin, glucagon and leptin, pro-inflammatory cytokines, such as IL-1β (interleukin-1β) and TNF-α (tumour necrosis factor-α), and lipids, including cholesterol and triacylglycerol (triglyceride), were all elevated in obese *w/lo* mice (Table 1), but the level of NEFAs (non-esterified fatty acids; 'free fatty acids') remained unchanged, suggesting obese *w/lo* mice have hyperinsulinaemia and moderate dyslipidaemia. However, unlike obese animal models, plasma adiponectin in obese *w/lo* mice was elevated.

Akin to insulin-resistant obese humans, obese *w/lo* mice are hyperinsulinaemic, yet they have lower random blood glucose than *w/w* controls (Figure 3C), suggesting their metabolism is unbalanced toward energy storage and that they remain insulin-responsive. Obese *w/lo* mice resemble MHO humans [3] in having slightly, yet significantly, elevated triacylglycerol and elevated leptin, but NEFAs and fasting glucose were not significantly elevated above normals. As with MHO and normal humans, but unlike insulin-resistant obese humans, *w/lo* mice retain a robust insulin-stimulated ability to dispose of glucose. The *w/lo* mice differ from MHO, obese and normal humans: none of these phenotypes have lower blood glucose. The lower 'random blood glucose' probably mimics a permanently fasting state, which may explain why the RER value of *w/lo* mice holds at a fasting level. It is widely accepted that low blood glucose is a strong hunger signal, which in *w/lo* mice probably provides a driving force for chronic hyperphagia. Therefore reduced Brd2 caused hyperinsulinaemia, but unalleviated low blood glucose in the fed state, and hyperadiponectinaemia, which are exceptionally rare in obese subjects.

Table 1 Blood chemistry and endocrine characteristics of *w/lo* and *w/w* mice at 9 months of age

P values were determined using Student's *t* test.

Parameter	*w/w*	*w/lo*	*P* value	*n*
Random plasma glucose (mg/dl)	161.8 ± 11.0	110.3 ± 20.0	2.1×10^{-5}	8
Fasting plasma glucose (mg/dl)	109.7 ± 18.5	88.1 ± 12.6	5.4×10^{-4}	11
Random plasma insulin (ng/ml)	1.5 ± 0.3	4.2 ± 0.7	3.2×10^{-5}	7
Fasting plasma insulin (ng/ml)	1.1 ± 0.4	3.2 ± 0.5	2.6×10^{-4}	7
Adiponectin (μg/ml)	20.9 ± 7.2	30.4 ± 5.1	8.8×10^{-3}	9
Leptin (ng/ml)	44.7 ± 18.7	132.0 ± 56.2	3.2×10^{-3}	9
Glucagon (pg/ml)	77.4 ± 24.5	108.2 ± 21.2	3.6×10^{-4}	9
NEFAs (mmol/l)	1.2 ± 0.2	1.4 ± 0.1	0.098	8
Cholesterol (mg/ml)	1.4 ± 0.4	2.0 ± 0.4	0.007	8
Triacylglycerol (mg/ml)	0.9 ± 0.2	1.2 ± 0.3	0.045	8
IL-1β (pg/ml)	30.0 ± 27.2	234.4 ± 164.3	0.047	4
TNF-α (pg/ml)	0.1 ± 0.1	10.8 ± 10.5	0.01	8

In obese animals, blood glucose tends to be above normal due to obesity-induced insulin resistance, which is a major cause of eventual β-cell failure and Type 2 diabetes. To explore glucose usage in obese *w/lo* mice, we performed IGTTs (intraperitoneal glucose tolerance tests): 1.5 g of D-glucose/kg of body weight was injected to challenge young (4 week) *w/lo* mice before obesity onset, older (40 week) *w/lo* mice with severe obesity and *w/w*

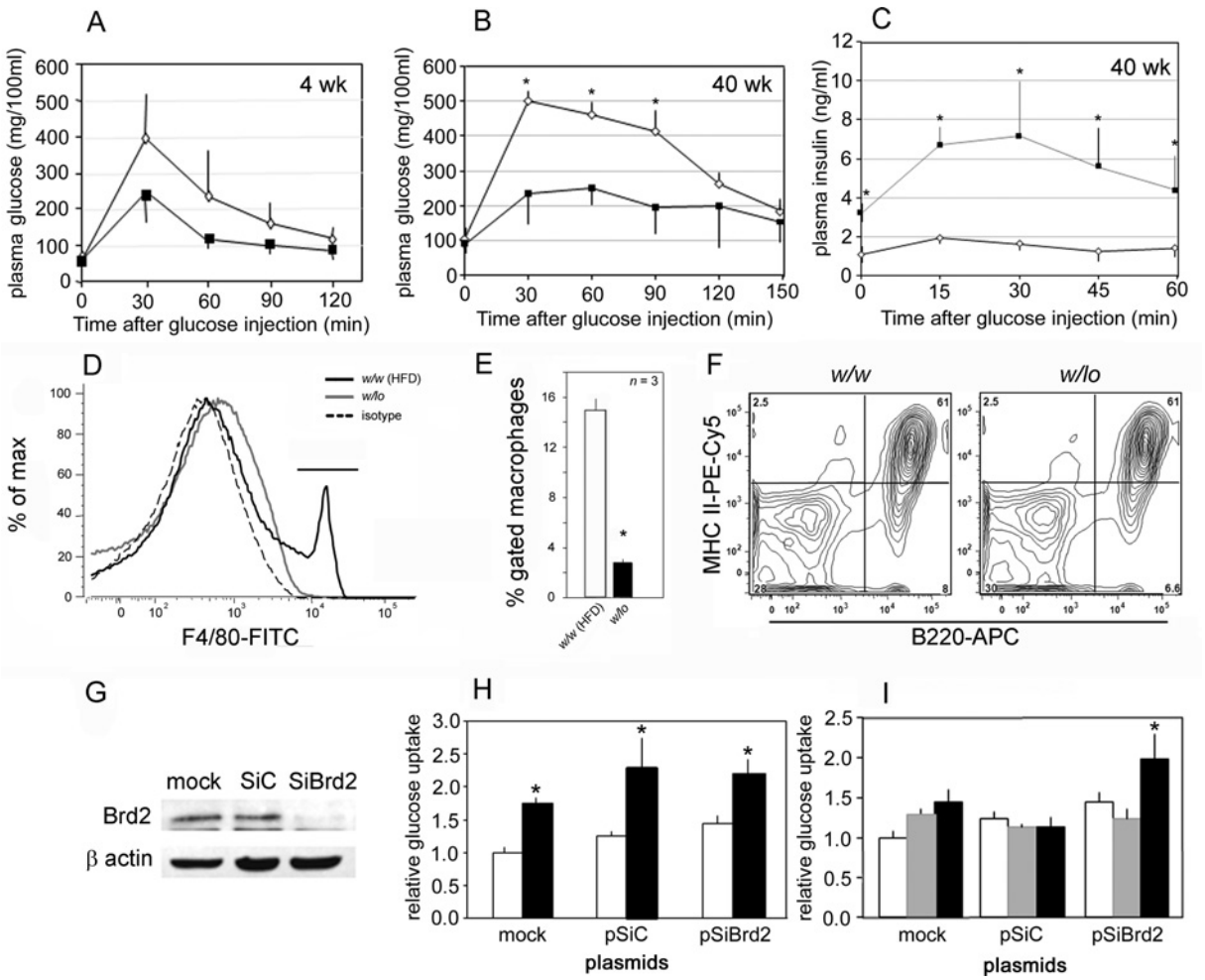

Figure 4 Reduced Brd2 enhances glucose tolerance *in vivo* and protects 3T3-L1 adipocytes from TNF-α-induced insulin resistance *in vitro*

IGTT (1.5 g of D-glucose/kg of body weight) in *w/w* mice (◇) and *w/lo* mice (■) at 4 weeks (**A**) and 40 weeks (**B**) of age. (**C**) Plasma insulin production during IGTT in *w/w* mice (◇) and *w/lo* mice (■). (**D**) Flow cytometry of F4/80$^+$ macrophages in the SVF isolated from the epididymal fat pad of obese *w/lo* mice (solid grey line) compared with obese *w/w* mice on a HFD [*w/w* (HFD)] as a positive control (solid black line) and isotype control (broken line). (**E**) Quantification of F4/80$^+$ macrophages. Open bar, obese *w/w* mice on a HFD [*w/w* (HFD)]; closed bar, obese *w/lo* mice. (**F**) Normal expression of MHC class II molecules [PE (phycoerythrin)-Cy5] on the surface of antigen-presenting B-cells (B220) from the spleens of *w/w* mice and *w/lo* mice; percentages of the gated lymphocytes are shown for each quadrant of the contour plot, as described previously [57]. (**G**) Immunoblot for Brd2 in 3T3-L1 pre-adipocytes stably transfected with Brd2 shRNA (SiBrd2) or control (SiC) plasmids. (**H**) Baseline (open bars) and insulin-stimulated (closed bars) glucose uptake by 3T3-L1 adipocytes. (**I**) Glucose uptake of 3T3-L1 adipocytes stably transfected with Brd2 or control shRNA plasmids and treated with 4 ng/ml TNF-α for 4 days to induce insulin resistance. Open bars, baseline; grey-shaded bars, TNF-α alone; closed bars, TNF-α+insulin. $n = 7$ in (**A**), $n = 4$ in (**B**, **C**, **H** and **I**), and $n = 3$ in (**E**); $^*P<0.05$.

controls. Interestingly, plasma glucose in both young and old *w/lo* mice only reached ~250 mg/dl and fell quickly to baseline in young mice. Conversely, plasma glucose in *w/w* mice rose to ~500 mg/dl and fell more slowly to baseline (Figures 4A and 4B). These results indicate that *w/lo* mice are more efficient at clearing glucose from the blood and more tolerant than *w/w* mice to glucose challenge during chronic obesity and even before the onset of obesity (Figure 2B). Insulin secretion during IGTT is much higher in *w/lo* mice than in *w/w* mice (Figure 4C). Taken together, these data make it clear that obese *w/lo* mice, although hyperinsulinaemic, do not progress to glucose intolerance and β-cell failure despite months of chronic obesity.

Reduced Brd2 levels block macrophage infiltration *in vivo* and insulin resistance *in vitro*

It is well established that chronic inflammation due to increased production of pro-inflammatory cytokines and adipose deposition in liver and muscle (two major targets of insulin action) cause insulin resistance in obesity and Type 2 diabetes [36]. Unexpectedly, despite their severe obesity, glucose intolerance was not observed in *w/lo* mice, although they have severe hepatosteatosis (Figure 2I) and elevated pro-inflammatory cytokines (Table 1). Furthermore, obese *w/lo* mice are more tolerant than *w/w* mice to a glucose challenge. These findings suggest inflammatory responses may be deficient in *w/lo* mice. We undertook additional experiments to explore the possibility that Brd2, as a signal transduction effector [13,14,17,19,28], might be required in normal cells to transduce signals from pro-inflammatory cytokines.

Macrophages and adipocytes release pro-inflammatory cytokines that can induce insulin resistance *in vitro* and *in vivo*, an important one of which is TNF-α [36]. Although *w/lo* mice have elevated serum TNF-α (Table 1), we were surprised to find that F4/80$^+$ (classically activated) inflammatory macrophages that might provide a source of TNF-α were missing from the SVF (stromal vascular fraction) of the epididymal fat depot of obese *w/lo* mice, although these macrophages

were nevertheless abundant in epididymal fat depots of *w*/*w* controls rendered obese by an HFD (Figure 4D; quantification is shown in Figure 4E). The lack of infiltration of fat in *w*/*lo* mice by these inflammatory cells probably provides another form of protection against insulin resistance in adipose tissues. Given the position of the *lacZ* disruption of the *Brd2* gene in RRT234 ES cells (Figure 1A), within the MHC class II locus, we performed control experiments to confirm that these mice did not have a global defect in antigen presentation that might provide a trivial explanation for immunodeficiency. The surface expression of MHC class II molecules was measured by flow cytometry of splenic B-cells from adult *w*/*lo* mice and was verified to be normal (Figure 4F). To test the hypothesis that whole-body reduction in Brd2 protects cells against cytokine-induced insulin resistance, Brd2 expression was reduced in the 3T3-L1 system by stable transfection of the pre-adipocytes with a plasmid encoding Brd2 shRNA (small-hairpin RNA) (pSiBrd2). Then the cells were differentiated to adipocytes with insulin/dexamethasone/isobutylmethylxanthine and pioglitazone. We confirmed that pSiBrd2 significantly reduced Brd2 protein in 3T3-L1 adipocytes (Figure 4G). The adipocytes were then treated with TNF-α and insulin-stimulated glucose uptake was measured. We found that knockdown of Brd2 itself had marginal effects on baseline and insulin-stimulated glucose uptake (Figure 4H). As expected, TNF-α inhibited insulin-stimulated glucose uptake in control cells, but cells with knocked-down Brd2 maintained their insulin sensitivity (Figure 4I). This result indicates that Brd2 is required for TNF-α signalling to induce insulin resistance *in vitro*.

Brd2 inhibits β-cell growth and insulin transcription

The hyperinsulinaemia and pancreatic islet expansion of obese animals and humans are usually considered to be compensatory responses of the organism to increased demand for insulin due to obesity-induced insulin resistance. Thus an interesting question arose: if obese *w*/*lo* mice are more tolerant to glucose challenge and have lower blood glucose than *w*/*w* mice, why do they still manifest hyperinsulinaemia and islet expansion? Given the role of Brd2 and its family of related proteins as cell-cycle and developmental regulators, we hypothesized first that β-cell proliferation might be uncoupled from glucose homoeostasis and β-cells might proliferate if Brd2 levels were reduced.

The long form of Brd2 is highly expressed in the pancreas of *w*/*w* mice (Figure 1B). We used indirect immunofluorescence to identify the cells of the pancreas that express Brd2 and found that Brd2 is exclusively expressed in islet β-cells, the insulin-producing cells of the pancreas (Figure 5A). This result suggested that β-cell function might be deregulated if Brd2 levels were reduced. We then hypothesized that, rather than a chronic manifestation of increased demand for insulin, the observed islet expansion in obese *w*/*lo* mice might be a driving force behind the obesity, if reduced Brd2 exerts a direct positive effect on β-cell mass.

Therefore we manipulated Brd2 expression in β-TC-6 cells, a murine insulinoma cell line, to model Brd2 function in β-cells. We stably transfected the cells with plasmids that express the long form of mouse Brd2 or Brd2 shRNA and counted cells over time (Figure 5B). Compared with controls, knockdown of Brd2 accelerated cell proliferation, but overexpression of Brd2 reduced cell proliferation and increased the number of dead cells (Figure 5D). Specifically, BrdU (bromodeoxyuridine) incorporation studies showed that knockdown of Brd2 promoted the entry into S-phase (Figure 5C; quantification is shown in Figure 5D). Conversely, overexpression of Brd2 reduced the number of cells entering S-phase and increased the number of sub-G_0/G_1 (presumably apoptotic) events (Figure 5D). These results suggest that the long form of Brd2 normally functions in β-cells to restrict β-cell proliferation, offering an interesting contrast with lymphoid cells and fibroblasts, in which ectopic expression of the short form of Brd2 promotes proliferation [14] and drives malignancy in Eμ-*Brd2* transgenic mice [28].

Given the function of Brd2 as a transcriptional co-regulator, its high expression in β-cells and the hyperinsulinaemia of *w*/*lo* mice, we next hypothesized that Brd2 is a co-repressor of insulin transcription [21]. Therefore we measured insulin mRNA levels in the transfected β-TC-6 cells with real-time RT (reverse transcription)–PCR. Knockdown of Brd2 increased insulin transcription in low-glucose medium (0.5 mM), but did not further increase insulin transcription stimulated by high-glucose medium (25 mM; Figure 5E). Conversely, overexpression of the long form of Brd2 (pmBrd2) inhibited insulin transcription in β-cells cultured in both low and high glucose (Figure 5E), which supports the hypothesis. Taken together, these results suggested that pancreatic islet expansion and hyperinsulinaemia in obese *w*/*lo* mice are not an adaptive response to glucose intolerance, but are direct consequences of reduced Brd2 levels in pancreatic β-cells. We therefore returned to young *w*/*lo* mice and gender-matched *w*/*w* mice at 8 weeks of age and examined their islets, before the onset of obesity. We found significant islet expansion (Figure 5F). The median number of β-cells per field of view of young *w*/*w* mouse islets was 50 cells (with 25 and 75 % percentiles of 33.5 and 83.5 cells; $n = 5$), but for young *w*/*lo* mouse islets the number was 222 cells (with 25 and 75 % percentiles of 191.2 and 579.0 cells; $n = 5$), which supports the hypothesis that islet expansion is a primary event in *w*/*lo* mice.

Brd2 knockdown promotes adipogenic differentiation *in vitro*

In obesity, adipocytes expand both in size and number to accommodate increased energy storage. Adipogenesis, the process by which adipocyte precursors develop into adipocytes, is regulated by a group of specific transcription factors. Because we found above that Brd2 probably functions as a co-repressor of insulin transcription, we wondered whether a similar co-repression mechanism might be at work in adipocytes. Thus we returned to the 3T3-L1 system. Pre-adipocytes were stably transfected with the same plasmids to overexpress or knockdown Brd2 (Figures 4 and 5), then adipogenic differentiation was induced with insulin/dexamethasone/isobutylmethylxanthine. We found that Brd2 knockdown promoted adipogenic differentiation, as shown qualitatively (Figure 6B) and quantitatively (Figure 6C); conversely, Brd2 overexpression strongly suppressed adipogenic differentiation (Figures 6B and 6C). In addition, Brd2 overexpression inhibited the induction of PPAR-γ (peroxisome-proliferator-activated receptor-γ) and ACC (acetyl-CoA carboxylase), two markers of adipogenesis (Figure 6E). These results suggest that Brd2 normally functions to inhibit adipogenic differentiation. Consistent with this interpretation, endogenous Brd2 expression in 3T3-L1 pre-adipocytes declines during adipogenic differentiation (Figure 6F). In control experiments, we confirmed that, in the presence of a PPAR-γ agonist (pioglitazone), wild-type 3T3-L1 pre-adipocytes differentiate as fully as pre-adipocytes in which Brd2 has been knocked down (see Supplementary Figure S1A available at http://www.BiochemJ.org/bj/425/bj4250071add.htm).

Brd2 co-represses PPAR-γ

PPAR-γ is the master regulator of adipogenesis and is regulated in part by multiprotein transcriptional complexes composed of

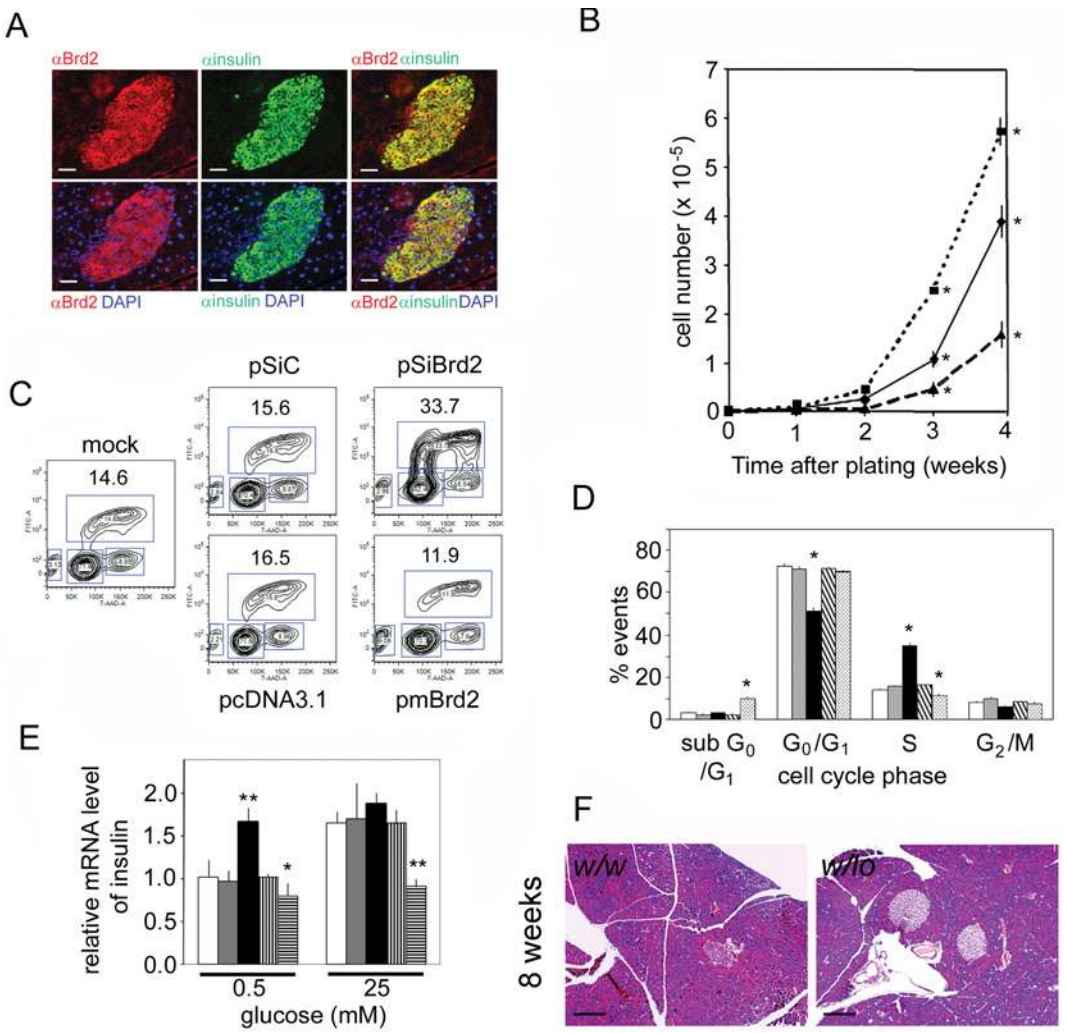

Figure 5 Brd2 regulates pancreatic β-cell biology

(**A**) Immunofluorescence images of a pancreatic islet from a 16-week-old *w*/*w* mouse stained with anti-Brd2 (αBrd2) and anti-insulin (αinsulin) antibodies, and DAPI (4′,6-diamidino-2-phenylindole) to visualize nuclei, showing β-cell-restricted expression. Scale bar, 50 μm. (**B**) Growth curves of β-TC-6 cells stably transfected with plasmids for overexpression of the long form of Brd2 (broken line), shRNA (dotted line) or control (solid line) as in Figure 4 ($n = 3$; $^*P<0.05$). (**C**) Representative BrdU assay of β-TC-6 cells stably transfected with plasmids as above. Percentages of cells in S-phase of the cell cycle are shown. (**D**) Quantification of flow cytometry results ($n = 3$; $^*P<0.05$). Open bar, mock; light-grey bar, pSiC; solid black bar, pSiBrd2 knockdown; coarse hatched bar, pcDNA control; fine hatched bar, pmBrd2 overexpression. (**E**) Real-time RT–PCR of insulin mRNA levels compared with β-actin in stably transfected β-TC-6 cells cultured in 0.5 or 25 mM glucose medium ($n = 3$; $^*P<0.05$ and $^{**}P<0.01$). Open bar, mock; light-grey bar, pSiC; closed bar, pSiBrd2 knockdown; vertical striped bar, pcDNA control; horizontal striped bar, pmBrd2 overexpression. (**F**) Pancreatic islets of *w*/*lo* mice and *w*/*w* mice at 8 weeks of age, before onset of obesity. Scale bar, 100 μm.

co-regulators. The activity of PPAR-γ is suppressed by a co-repressor protein complex before being activated. Upon activation through ligand binding, a co-activator complex replaces the inhibitory co-repressor complex. We have previously characterized Brd2-associated transcriptional protein complexes and reported that, among other factors, such complexes contain Hats/Hdacs and nucleosome remodelling factors, including members of the SWI/SNF complex [18]. These transcriptional co-factors are also found in the protein complexes that co-regulate PPAR-γ transcriptional activity [37]. Thus we hypothesized that Brd2-dependent complexes and PPAR-γ-dependent complexes share overlapping composition and activities (Figure 6A) and that Brd2 opposes PPAR-γ action as a direct co-repressor. It follows first that Brd2 and PPAR-γ should associate with each other. Therefore we performed protein co-immunoprecipitation of Brd2 and PPAR-γ with cell lysates from 3T3-L1 adipocytes 3 days after induction of differentiation, when Brd2 and PPAR-γ are co-expressed (Figure 6F). We found that Brd2 associates with PPAR-γ *in vitro* in a ligand-independent fashion (Figure 6G). To determine whether the binding of Brd2 and PPAR-γ regulates PPAR-γ transcriptional activity, 3T3-L1 pre-adipocytes were transiently transfected with a luciferase reporter plasmid that contains a triplicated PPAR-responsive element (PPRE-3X-Luc), pPPAR-γ, *Renilla* luciferase and effector plasmids (pSiBrd2, pmBrd2 and controls); then luciferase activity was measured. We found that reduced Brd2 expression increased PPAR-γ transcriptional activity, whereas increased Brd2 expression reduced PPAR-γ transcriptional activity (Figure 6H). These results suggest that Brd2 acts as a PPAR-γ co-repressor; Brd2 knockdown increases PPAR-γ activity and facilitates adipogenesis, consistent with the dramatically increased adipose tissue burden of *w*/*lo* mice.

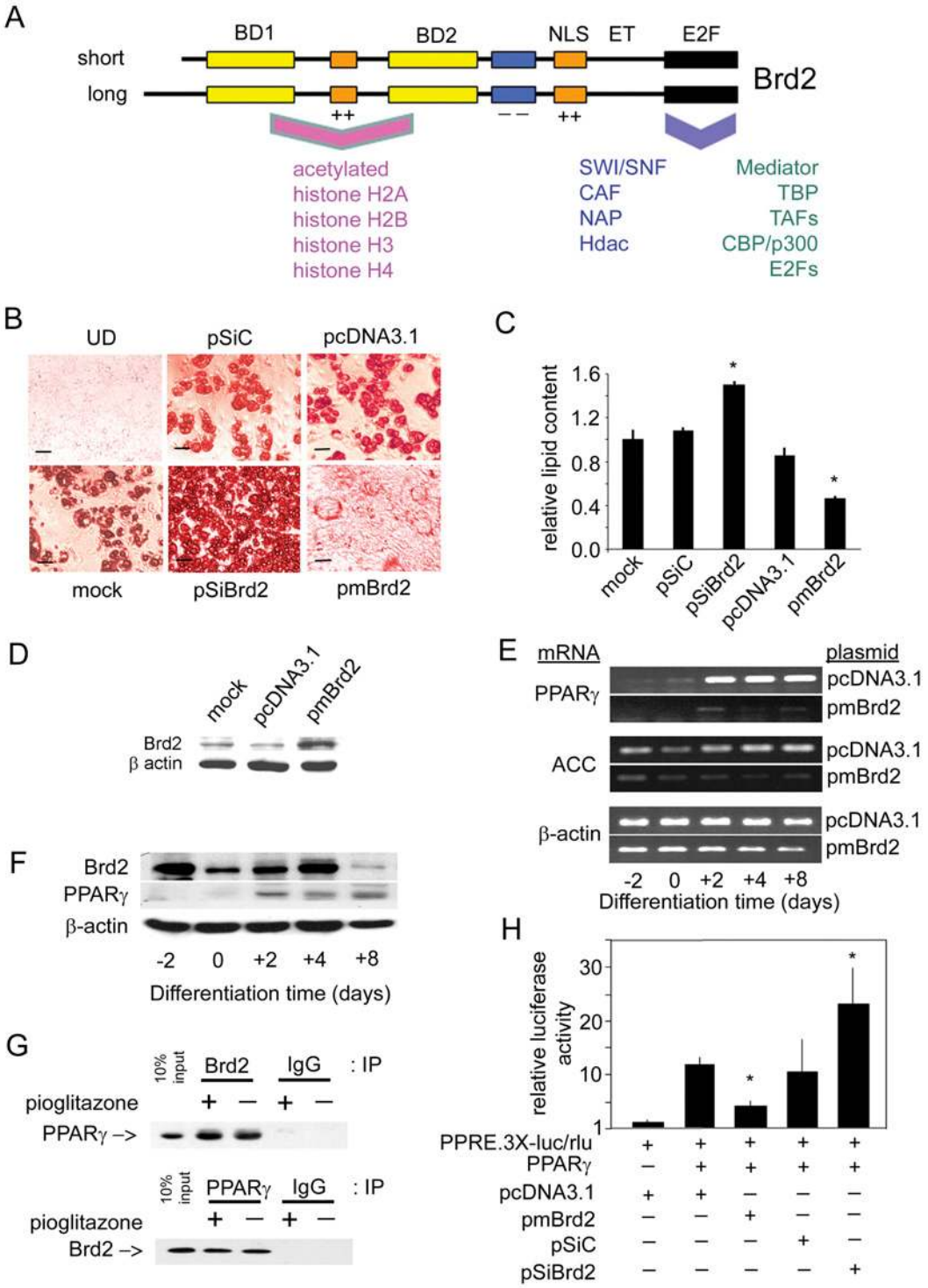

Figure 6 Brd2 inhibits adipogenic differentiation and co-represses PPAR-γ transcription

(**A**) Schematic of Brd2 structure [4,14] and reported interacting proteins [18,19]. BD, bromodomain; NLS, nuclear localization signal; ET, extraterminal domain; E2F, E2F-complex association domain [19]; ++, basic domain; – –, acidic domain. Human and mouse Brd2 proteins are approx. 91 % identical. Associated proteins are discussed in the Introduction. CAF, chromatin assembly factor; NAP, nucleosome assembly protein. (**B**) Manipulation of Brd2 in 3T3-L1 adipocytes with Brd2 shRNA, Brd2 overexpression or controls. Oil Red O staining visualizes lipid content in cells that have undergone adipogenic differentiation. Adipogenic differentiation of 3T3-L1 adipocytes from pre-adipocytes was performed as described previously [58]. UD, undifferentiated (see the legend to Figure 4 for plasmid abbreviations). (**C**) Quantification of lipid content in transfected 3T3-L1 cells after adipogenic differentiation ($n = 3$; $^*P < 0.05$). Lipid content using Oil Red O stain was determined as described previously [59]. (**D**) Immunoblot analysis verifies increased Brd2 expression in 3T3-L1 pre-adipocytes transfected with pmBrd2 or controls. (**E**) Overexpression of Brd2 with pmBrd2 suppresses normal expression of two adipogenic markers, PPAR-γ and ACC, as detected by RT–PCR at different time points during adipogenic differentiation. (**F**) Kinetics of Brd2 and PPAR-γ expression in 3T3-L1 pre-adipocytes during adipogenesis. (**G**) Co-immunoprecipitation (IP) of Brd2 and PPAR-γ in 3T3-L1 cells 3 days after induction of differentiation. IgG, non-specific control. (**H**) Brd2 inhibits PPAR-γ activity, as assessed by transcriptional activity of a PPAR-γ-driven luciferase reporter in 3T3-L1 pre-adipocytes, in response to manipulation of Brd2 ($n = 3$; $^*P <$ 0.05).

DISCUSSION

The newly described bromodomain protein Brd2 performs profound, diverse and non-redundant functions in the life of specialized cells. Although elevated expression of Brd2 has been linked to cancer, the broader normal functions of the ubiquitous double bromodomain-containing BET class of transcriptional co-regulators are not well understood. In mice, knockout of the closely related gene *Brd4* is lethal, and haploinsufficiency poses severe problems for cell cycle and organ development [32]. Clues from studies of the yeast single bromodomain homologues *BDF1* and *BDF2*, and the *Drosophila* homologue *fsh*, imply that these proteins function as chromatin-directed developmental regulators with maternal effects in animals [24,27]. Bromodomain-containing protein complexes respond to signal transduction to mediate protein–protein interactions among TAFs, histone-modification enzymes and the chromatin remodelling machinery at specific promoters during development and in differentiated cells of the adult, thereby establishing repressive or transcriptionally active chromatin. Such a broad mechanism makes it difficult to establish specific paradigms for action on target genes or to predict how mutations cause specific diseases; we suspect that *brd2* mutations functionally resemble *swi*/*snf* mutations in their networked pleiotropic effects [20]. Our attempts to generate a Brd2-knockout mouse line with RRE050, a *Brd2* gene-trapped murine ES cell-line failed, consistent with Brd4 knockout attempts [32]. Shang et al. [33] found that *brd2*$^{(-/-)}$-null embryos derived from RRE050 ES cells showed a phenotype different from *brd4*$^{(-/-)}$-null embryos; they hypothesized a deficiency in neuronal differentiation and brain development. This phenotype has been confirmed very recently [34]. However, our gene disruption in the 5′ region of the *Brd2* gene in the ES cell line RRT234, which reduced rather than eliminated *Brd2* gene expression, overcame problems of early lethality to give *w*/*lo* mice. The unexpected severely obese phenotype of the *w*/*lo* mice indicates that, among other functions, Brd2 in mammals is also a regulator of energy balance. The body weights that adult *w*/*lo* mice attain (Figure 2B) are among the highest reported for obese mouse models and rival adiponectin transgenic mice on the *ob*/*ob* background [38]. Surprisingly, *w*/*lo* mice have long lives (~20 months) despite their obesity and do not appear to die of tumours, haematological or immunological abnormalities, opportunistic infections, pulmonary disease or musculoskeletal disorders. The discovery of these mice was completely serendipitous and could not have been anticipated from the ES cells we used.

The *w*/*lo* mice pose two problems. First, why do they gain weight with a well-defined mutation located in a gene not previously thought to play any role in energy metabolism? Secondly, upon development of severe obesity, why does the same mutation protect them from the development of Type 2 diabetes, which marks a major departure from numerous other mouse models of obesity?

In animals, insulin is the major regulator of anabolism. Maintenance of proper β-cell mass is crucial for energy homoeostasis [39], and failure of β-cell production of insulin is a characteristic defect in both Type 1 and Type 2 diabetes. In most obese animals, hyperinsulinaemia and β-cell expansion are compensatory for insulin resistance. Pancreatic β-cell mass is regulated by at least four independent mechanisms: β-cell apoptosis, β-cell replication by mitosis, β-cell size and β-cell neogenesis from pancreatic progenitors. The issue of whether the reduction in human β-cell mass in diabetes results from increased β-cell apoptosis, reduced β-cell neogenesis/replication, or both factors, remains unresolved [40]. However, recent evidence indicates that maintenance of β-cell mass in young adult mice is primarily due to β-cell replication [41]; proper control of proliferation is critical to maintain sufficient β-cells to produce enough insulin. The transition from G_1- to S-phase of the cell cycle is controlled by the D-type cyclins in conjunction with E2Fs, cyclin-dependent kinases and their inhibitors, which are important for β-cell growth; if D-type cyclin activity falls below a critical level, β-cell mitogenesis is almost totally ablated [42].

The expression of different forms of Brd2 varies significantly among mouse tissues (Figure 1B), with the long form of Brd2 highly expressed in β-cells (Figure 5A). We have established previously that the short form of Brd2 is a pro-mitotic factor in lymphoid cells [28], through its transcriptional activation of E2F-dependent cyclin genes, including *cyclin D1* [19]. β-Cell expansion and hyperinsulinaemia in obese *w*/*lo* mice appear to be uncoupled from hyperglycaemia, which suggests Brd2 plays a direct non-sensing role in the regulation of β-cell mass and insulin production. We tested this hypothesis *in vitro* in β-TC-6 cells, where knockdown of Brd2 forces more cells into S-phase and promotes proliferation, which suggests that the long form of Brd2 normally acts as a negative regulator of the G_1 checkpoint, to oppose β-cell mitogenesis and thus restrict β-cell mass. Hyperinsulinaemia in the absence of glucose intolerance creates chronic lower blood glucose; glucose is rapidly cleared from the blood and stored as fat. Thus we interpret *w*/*lo* mice: chronic hyperphagia addresses their low blood glucose, but in the absence of increased physical activity to balance increased storage they become obese.

Adipogenesis is also crucial for energy balance. Deregulated adipogenesis can cause lipoatrophy or obesity; both are harmful. A group of transcription factors, such as PPAR-γ and C/EPBα (CCAAT enhancer-binding protein-α), play critical roles in this process, especially PPAR-γ: its function is necessary and probably sufficient for adipogenesis [43]. Interestingly, Brd2 protein expression is high in pre-adipocytes and falls to barely detectable amounts in differentiated adipocytes, which suggested to us that Brd2 might normally function as a negative regulator of the adipogenic differentiation programme, possibly as a transcriptional co-repressor of PPAR-γ. The activity of PPAR-γ is regulated by ligands and transcriptional co-regulators. We found that Brd2 binds to PPAR-γ *in vitro* and this binding cannot be reversed by the PPAR-γ agonist pioglitazone. Furthermore, the long form of Brd2 inhibits PPAR-γ transcriptional activity, which we interpret as an explanation for the increased adipogenic differentiation in 3T3-L1 cells with knocked-down Brd2. In this respect, Brd2 functionally resembles another chromatin-directed transcriptional co-regulator, Adp, which has been reported to bind histones and Hdac3, thus inhibiting PPAR-γ activity and adipogenesis [44]. We speculate that the increased energy storage brought about by elevated insulin works together with reduced co-repression of PPAR-γ-driven adipogenesis to promote severe obesity in *w*/*lo* mice.

Key factors also clearly protect obese *w*/*lo* mice from glucose intolerance. The RER results suggest constant lipid oxidation reduces fat accumulation, but this pathway is insufficient to prevent severe obesity. Normally, chronic hyperglycaemia and increased blood NEFAs in obesity impair β-cell function through nutrient-induced β-cell apoptosis. The reduced feeding blood glucose and normal NEFA levels in obese *w*/*lo* mice probably preserve β-cells in these mice. Interestingly, obese *w*/*lo* phenocopy mice that harbour a β-cell-restricted deletion of *Pten* (encoding phosphatase and tensin homologue deleted on chromosome 10), which clear injected glucose better than wild-type mice and have increased islet numbers and total mass of islets, as well as having lower fasting blood glucose and resistance to

β-cell apoptosis [45], suggesting that Brd2 may be a transcriptional effector of the Pten/Akt pathway in β-cells.

Furthermore, adiponectin, an important adipokine, is probably relevant in this model. Adiponectin is a protective insulin-sensitizing factor that can temper obesity-induced insulin resistance [46]. But a paradox has been noted: in most obese animals, including humans, an increased number of adipocytes ought to produce more adiponectin; however, observed levels of adiponectin are in fact lower. It is likely that insulin resistance plays a role in this phenomenon, reducing blood adiponectin and *vice versa*, thus forming a 'vicious circle' of diminished adiponectin [47]. Interestingly, unlike in other animal models of obesity, the plasma adiponectin level in obese *w/lo* mice is increased (31.3 ± 3.0 μg/ml), thus it is reasonable to attribute superior glucose sensitivity in obese *w/lo* mice partly to their elevated adiponectin; hyperadiponectinaemia is associated with improved metabolic profiles of obese patients [48]. This serum adiponectin concentration matches the hyperadiponectinaemia of male adiponectin transgenic mice [49]; approximately half this concentration is sufficient to rescue *ob/ob* mice from Type 2 diabetes [38]. It will be important to determine whether Brd2 normally co-represses adiponectin transcription, similar to its action on insulin transcription and the PPAR-γ-dependent promoter we tested. Scherer and co-workers have noted an interesting 'feed-forward' relationship between PPAR-γ agonist action and hyperadiponectinaemia [38]. Given the evidence that Brd2 reduction phenocopies thiazolidinedione action, promoting adipogenesis, it is possible that the transcriptional activity of Brd2 provides a functional link between the two processes.

Finally, it is well established that production of pro-inflammatory cytokines from adipose cells accumulated in liver and muscle during obesity promotes insulin resistance [50]. Unexpectedly, despite their severe obesity, increased serum levels of pro-inflammatory cytokines, such as TNF-α and IL-1β, hepatosteatosis and highly elevated transcription of these cytokine genes in WAT (white adipose tissue; see Supplementary Figure S1B), obese *w/lo* mice are more tolerant than *w/w* mice to glucose challenge; blood glucose levels in both the fed state and during an IGTT fall short of the levels attained in *w/w* mice. Interestingly, *aP2* (adipocyte fatty acid-binding protein 4)-deficient mice appear to uncouple dietary obesity from insulin resistance in part through failure of TNF-α production [51], yet we encountered a surprise while investigating fat depots: adipose tissue of obese *w/lo* mice lack infiltration by F4/80$^+$ inflammatory macrophages (Figure 4D), a phenotype previously reported for adiponectin transgenic mice [38]. It is currently unclear whether this lack of macrophage recruitment is a specific consequence of elevated serum adiponectin or a lack of adipocyte necrosis; unlike adiponectin transgenic mice, obese *w/lo* mice have adipocyte hypertrophy but not hyperplasia. Furthermore, *in vitro* glucose uptake experiments with 3T3-L1 adipocytes reveal that Brd2 is required for TNF-α-induced insulin resistance. Thus (i) elevated adiponectin, (ii) increased BAT and elevated uncoupling proteins, (iii) high quality adipose tissue without infiltration by inflammatory cells, and (iv) molecular uncoupling of elevated TNF-α signalling from insulin resistance work together to protect obese *w/lo* mice from eventual Type 2 diabetes.

Certain naturally occurring genetic environments, such as MHO or MONW human subpopulations [3], uncouple obesity from the insulin resistance and Type 2 diabetes commonly found in the general population, thus a substantial fraction of obese patients avoid insulin resistance. There is intense interest in obtaining greater mechanistic understanding of the genes involved, first to deepen our understanding of the basic biology of insulin resistance and secondly to identify possible therapeutic targets. The location of the *BRD2* gene within the MHC class II locus of both humans and mice, situated among genes devoted to antigen presentation but itself unrelated to them, nevertheless suggests intriguing links to the immune system, particularly to inflammation. The lack of development of inflammation-associated glucose intolerance in these mice is unlikely to be due to a global deficiency in antigen presentation, because *lacZ* gene disruption of the *Brd2* gene in RRT234 ES cells did not impair expression of MHC class II molecules in the periphery. Immune and metabolic systems are closely related, developmentally and functionally, and disorders in the immune system are associated with obesity and diabetes [52]. Although Brd2 expression in the adult mouse brain is low, it remains possible that Brd2 in the brain plays a role in the regulation of energy metabolism; however, given the chromosomal location of the *BRD2* gene at 6p21.3, we nevertheless favour a role in immunity and inflammation. Our present data suggest that lowered levels of Brd2 reduce inflammatory signal transduction, which lead us to speculate that the reduced inflammatory profile of MHO humans might be related to polymorphism at the *BRD2* locus. There are no published studies of such polymorphisms at the time of writing.

We speculate further that the strong influence of Brd2 levels on insulin production and action suggest Brd2 is probably a promising target for diabetes treatment, but also imply that overactive Brd2 might cause diabetes. Interestingly, the MHC class II in humans is the most strongly linked locus to Type 1 diabetes [53]. The molecular mechanisms of this phenomenon are still not fully understood. 'Islet insult' or β-cell death is probably required for the aetiology of Type 1 diabetes. Notably, Brd2 not only regulates β-cell growth and insulin transcription *in vitro*, but overexpression of Brd2 also increases the number of apoptotic cells (Figure 5D), which, together with the potential role of Brd2 in the immune system, suggests further studies to investigate a possible role of Brd2 in the aetiology of Type 1 diabetes.

Body energy balance is regulated by a complex network of signals from both inside and outside of the body. More than 100 genes have been implicated in body weight regulation [54]. Emerging evidence reveals critical roles for transcriptional co-regulators in energy balance, such as PGC-1, a PPAR-γ co-activator, which controls energy storage and expenditure by regulating the development and function of adipose tissue, skeletal muscle and liver [55]. Similarly, PRDM16 (PR-domain-containing lb) interacts with the transcriptional co-regulators PGC-1α and PGC-1β to control an important differentiation switch between BAT and skeletal muscle [56]. Thus specific MDa complexes of transcription-factor-associated co-regulators are essential for proper control of energy metabolism. We suggest Brd2 and its associated protein complexes should be included in this group of transcriptional co-regulators that control energy balance.

AUTHOR CONTRIBUTION

Fangnian Wang performed most of the experiments with the necessary assistance of Hongsheng Liu, Wanda Blanton and Anna Belkina, who helped Fangnian Wang with the flow cytometry. Nathan LeBrasseur performed body composition, calorimetry and respiratory exchange ratio measurements. Fangnian Wang wrote a first draft of the paper, and all authors consulted on the final version. Gerald Denis conceptualized the project, directed the experiments, contributed to the calculation of the statistics, finalized the paper and wrote the grants that provided funding.

ACKNOWLEDGEMENTS

We note the National Institutes of Health sponsorship of both the National Heart Lung and Blood Institute –BayGenomics, and the National Center for Research Resources –

Mutant Mouse Regional Resource Center, and we thank the Murine Targeted Genomics Laboratory at the University of California, Davis, CA, U.S.A. We also thank H. Li (Joslin Diabetes Center, Boston, MA, U.S.A.) for serological assays; Z. Arany (Brigham and Women's Hospital, Boston, MA, U.S.A); and the Transgenic Core Facility, Flow Cytometry Core Facility and M. Kelly of the Section of Endocrinology, Diabetes and Nutrition (all at Boston University School of Medicine) for joint projects, helpful discussion and reagents. We thank B. Corkey, S. Farmer, S. Fried, P. Pilch, N. Ruderman and other members of the Boston Obesity Nutrition Research Center (P30 DK046200) for useful discussions. We thank D. Faller, A. Sinha and other members of the Cancer Research Center for invaluable help and support. This paper is dedicated to the memory of Edward M. Kennedy, United States Senator for Massachusetts, who was an ardent supporter of Boston Medical Center and its mission.

FUNDING

This work was supported by grants from the American Cancer Society; the National Institutes of Health [grant number T32 AI007309]; and pilot funds awarded to G.V.D. from the Boston Area Diabetes Endocrinology Research Center [grant number P30 DK057521].

REFERENCES

1 Zimmet, P., Alberti, K. G. and Shaw, J. (2001) Global and societal implications of the diabetes epidemic. Nature **414**, 782–787
2 Wild, S., Roglic, G., Green, A., Sicree, R. and King, H. (2004) Global prevalence of diabetes: estimates for the year 2000 and projections for 2030. Diabetes Care **27**, 1047–1053
3 Succurro, E., Marini, M. A., Frontoni, S., Hribal, M. L., Andreozzi, F., Lauro, R., Perticone, F. and Sesti, G. (2008) Insulin secretion in metabolically obese, but normal wt, and in metabolically healthy but obese individuals. Obesity **16**, 1881–1886
4 Beck, S., Hanson, I., Kelly, A., Pappin, D. J. C. and Trowsdale, J. (1992) A homologue of the *Drosophila female sterile homeotic* (*fsh*) gene in the class II region of the human MHC. DNA Seq. **2**, 203–210
5 Salter-Cid, L., Pasquier, L. and Flajnik, M. (1996) RING3 is linked to the *Xenopus* major histocompatibility complex. Immunogenetics **44**, 397–399
6 Ting, J. P. and Trowsdale, J. (2002) Genetic control of MHC class II expression. Cell **109**, S21-S33
7 Florence, B. and Faller, D. V. (2001) You bet-cha: a novel family of transcriptional regulators. Front. Biosci. **6**, D1008–D1018
8 Zeng, L. and Zhou, M. M. (2002) Bromodomain: an acetyl-lysine binding domain. FEBS Lett. **513**, 124–128
9 Denis, G. V. (2001) Bromodomain motifs and "scaffolding"? Front. Biosci. **6**, D1065–D1068
10 LeRoy, G., Rickards, B. and Flint, S. J. (2008) The double bromodomain proteins Brd2 and Brd3 couple histone acetylation to transcription. Mol. Cell **30**, 51–60
11 Tamkun, J. W., Deuring R., Scott M. P., Kissenger, M., Pattatucci, A. M., Kaufman, T. C. and Kennison, J. A. (1992) *brahma*: a regulator of *Drosophila* homeotic genes structurally related to the yeast transcriptional activator SWI2/SNF2. Cell **68**, 561–572
12 Wang, W., Côte, J., Xue, Y., Zhou, S., Khavari, P. A., Biggar, S. R., Muchardt, C., Kalpana, G. V., Goff, S. P., Yaniv, M., Workman, J. L. and Crabtree, G. R. (1996) Purification and biochemical heterogeneity of the mammalian SWI-SNF complex. EMBO J. **15**, 5370–5382
13 Denis, G. V. and Green, M. R. (1996) A novel, mitogen-activated nuclear kinase is related to a *Drosophila* developmental regulator. Genes Dev. **10**, 261–271
14 Sinha, A., Faller, D. V. and Denis, G. V. (2005) Bromodomain analysis of Brd2-dependent transcriptional activation of *cyclin A*. Biochem. J. **387**, 257–269
15 Thorpe, K. L. and Beck, S. (1998) DNA sequence and structure of the mouse RING3 gene: identification of variant RING3 transcripts. Immunogenetics **48**, 82–86
16 Nakamura, Y., Umehara, T., Nakano, K., Jang, M. K., Shirouzu, M., Morita, S., Uda-Tochio, H., Hamana, H., Terada, T., Adachi, N. et al. (2007) Crystal structure of the human *BRD2* bromodomain: insights into dimerization and recognition of acetylated histone H4. J. Biol. Chem. **282**, 4193–4201
17 Kornberg, R. D. (2005) Mediator and the mechanism of transcriptional activation. Trends Biochem. Sci. **30**, 235–239
18 Denis, G. V., McComb, M. E., Faller, D. V., Sinha, A., Romesser, P. B. and Costello, C. E. (2006) Identification of transcription complexes that contain the double bromodomain protein Brd2 and chromatin remodeling machines. J. Proteome Res. **5**, 502–511
19 Denis, G. V., Vaziri, C., Guo, N. and Faller, D. V. (2000) RING3 kinase transactivates promoters of cell cycle regulatory genes through E2F. Cell Growth. Differ. **11**, 417–424
20 Holstege, F. C., Jennings, E. G., Wyrick, J. J., Lee, T. I., Hengartner, C. J., Green, M. R., Golub, T. R., Lander, E. S. and Young, R. A. (1998) Dissecting the regulatory circuitry of a eukaryotic genome. Cell **95**, 717–728
21 Denis, G. V. (2001) Duality in bromodomain-containing protein complexes. Front. Biosci. **6**, D849–D852
22 Chua, P. and Roeder, G. S. (1995) Bdf1, a yeast chromosomal protein required for sporulation. Mol. Cell. Biol. **15**, 3685–3696
23 Matangkasombut, O., Buratowski, R. M., Swilling, N. W. and Buratowski, S. (2000) Bromodomain factor 1 corresponds to a missing piece of yeast TFIID. Genes Dev. **14**, 951–962
24 Matangkasombut, O. and Buratowski, S. (2003) Different sensitivities of bromodomain factors 1 and 2 to histone H4 acetylation. Mol. Cell **11**, 353–363
25 Chang, Y. L., King, B., Lin, S. C., Kennison, J. A. and Huang, D. H. (2007) A double-bromodomain protein, FSH-S, activates the homeotic gene *Ultrabithorax* through a critical promoter-proximal region. Mol. Cell. Biol. **27**, 5486–5498
26 Mozer, B. A. and Dawid, I. B. (1989) Cloning and molecular characterization of the *trithorax* locus of *Drosophila melanogaster*. Proc. Natl. Acad. Sci. U.S.A. **86**, 3738–3742
27 Digan, M. E., Haynes, S. R., Mozer, B. A., Dawid, I. B., Forquignon, F. and Gans, M. (1986) Genetic and molecular analysis of *fs(1)h*, a maternal effect homeotic gene in *Drosophila*, Dev. Biol. **114**, 161–169
28 Greenwald, R., Tumang, J. R., Sinha, A., Currier, N., Cardiff, R. D., Rothstein, T. L., Faller, D. V. and Denis, G. V. (2004) Eμ-*BRD2* transgenic mice develop B cell lymphoma and leukemia. Blood **103**, 1475–1484
29 Wu, S. Y. and Chiang, C. M. (2007) The double bromodomain-containing chromatin adaptor Brd4 and transcriptional regulation. J. Biol. Chem. **282**, 13141–13145
30 Dey, A., Chitsaz, F., Abbasi, A., Misteli, T. and Ozato, K. (2003) The double bromodomain protein Brd4 binds to acetylated chromatin during interphase and mitosis. Proc. Natl. Acad. Sci. U.S.A. **100**, 8758–8763
31 Dey, A., Ellenberg, J., Farina, A., Coleman, A. E., Maruyama, T., Sciortino, S., Lippincott-Schwartz, J. and Ozato, K. (2000) A bromodomain protein, MCAP, associates with mitotic chromosomes and affects G_2-to-M transition. Mol. Cell. Biol. **20**, 6537–6549
32 Houzelstein, D., Bullock, S. L., Lynch, D. E., Grigorieva, E. F., Wilson, V. A. and Beddington, R. S. P. (2002) Growth and early postimplantation defects in mice deficient for the bromodomain-containing protein Brd4. Mol. Cell. Biol. **22**, 3794–3802
33 Shang, E., Wang, X., Wen, D., Greenberg, D. A. and Wolgemuth, D. J. (2009) Double bromodomain-containing gene *Brd2* is essential for embryonic development in mouse. Dev. Dyn. **238**, 908–917
34 Gyuris, A., Donovan, D. J., Seymour, K. A., Lovasco, L. A., Smilowitz, N. R., Halperin, A. L., Klysik, J. E. and Freiman, R. N. (2009) The chromatin-targeting protein Brd2 is required for neural tube closure and embryogenesis. Biochim. Biophys. Acta **1789**, 413–421
35 Tomita, T., Doull, V., Pollock, H.G. and Krizsan, D. (1992) Pancreatic islets of obese hyperglycemic mice (*ob*/*ob*) Pancreas **7**, 367–357
36 Kroder, G., Bossenmaier, B., Kellerer, M., Capp, E., Stoyanov, B., Mühlhöfer, A., Berti, L., Horikoshi, H., Ullrich, A. and Häring, H. (1996) Tumor necrosis factor-α- and hyperglycemia-induced insulin resistance. Evidence for different mechanisms and different effects on insulin signaling. J. Clin. Invest. **97**, 1471–1477
37 Rosen, E. D., Walkey, C. J., Puigserver, P. and Spiegelman, B. M. (2000) Transcriptional regulation of adipogenesis. Genes Dev. **14**, 1293–1307
38 Kim, J. Y., van de Wall, E., Laplante, M., Azzara, A., Trujillo, M. E., Hofmann, S. M., Schraw, T., Durand, J. L., Li, H., Li, G. et al. (2007) Obesity-associated improvements in metabolic profile through expansion of adipose tissue. J. Clin. Invest. **117**, 2621–2637
39 Kahn, S. E. (2000) The importance of the β-cell in the pathogenesis of type 2 diabetes mellitus. Am. J. Med. **108**, (Suppl. 6a), 2S–8S
40 Rhodes, C. J. (2005) Type 2 diabetes: a matter of β-cell life and death? Science **307**, 380–384
41 Dor, Y., Brown, J., Martinez, O. I. and Melton, D. A. (2004) Adult pancreatic β-cells are formed by self-duplication rather than stem-cell differentiation. Nature **429**, 41–46
42 Kushner, J. A., Ciemerych, M. A., Sicinska, E., Wartschow, L. M., Teta, M., Long, S. Y., Sicinski, P. and White, M. F. (2005) Cyclins D2 and D1 are essential for postnatal pancreatic β-cell growth. Mol. Cell. Biol. **25**, 3752–3762
43 Rosen, E. D., Sarraf, P., Troy, A. E., Bradwin, G., Moore, K., Milstone, D. S., Spiegelman, B. M. and Mortensen, R. M. (1999) PPARγ is required for the differentiation of adipose tissue *in vivo* and *in vitro*. Mol. Cell **4**, 611–617
44 Suh, J. M., Zeve, D., McKay, R., Seo, J., Salo, Z., Li, R., Wang, M. and Graff, J. M. (2007) Adipose is a conserved dosage-sensitive antiobesity gene. Cell Metab. **6**, 195–207
45 Stiles, B. L., Kuralwalla-Martinez, C., Guo, W., Gregorian, C., Wang, Y., Tian, J., Magnuson, M. A. and Wu, H. (2006) Selective deletion of Pten in pancreatic β-cells leads to increased islet mass and resistance to STZ-induced diabetes. Mol. Cell. Biol. **26**, 2772–2781
46 Guerre-Millo, M. (2008) Adiponectin: an update. Diabetes Metab. **34**, 12–18
47 Weyer, C., Funahashi, T., Tanaka, S., Hotta, K., Matsuzawa, Y., Pratley, R. E. and Tataranni, P. A. (2001) Hypoadiponectinemia in obesity and type 2 diabetes: close association with insulin resistance and hyperinsulinemia. J. Clin. Endocrinol. Metab. **86**, 1930–1935

48 Côté, M., Mauriège, P., Bergeron, J., Alméras, N., Tremblay, A., Lemieux, I. and Després, J. P. (2005) Adiponectinemia in visceral obesity: impact on glucose tolerance and plasma lipoprotein and lipid levels in men. J. Clin. Endocrinol. Metab. **90**, 1434–1439
49 Combs, T. P., Pajvani, U. B., Berg, A. H., Lin, Y., Jelicks, L. A., Laplante, M., Nawrocki, A. R., Rajala, M. W., Parlow, A. F., Cheeseboro, L. et al. (2004) A transgenic mouse with a deletion in the collagenous domain of adiponectin displays elevated circulating adiponectin and improved insulin sensitivity. Endocrinology **145**, 367–383
50 Shoelson, S. E., Herrero, L. and Naaz, A. (2007) Obesity, inflammation, and insulin resistance. Gastroenterology **132**, 2169–2180
51 Hotamisligil, G. S., Johnson, R. S., Distel, R. J., Ellis, R., Papaioannou, V. E. and Spiegelman, B. M. (1996) Uncoupling of obesity from insulin resistance through a targeted mutation in aP2, the adipocyte fatty acid binding protein. Science **274**, 1377–1379
52 Hotamisligil, G. S. (2006) Inflammation and metabolic disorders. Nature **444**, 860–867
53 Jahromi, M. M. and Eisenbarth, G. S. (2006) Genetic determinants of type 1 diabetes across populations. Ann. N.Y. Acad. Sci. **1079**, 289–299
54 Leibel, R. L. (2008) Energy in, energy out, and the effects of obesity-related genes. N. Engl. J. Med. **359**, 2603–2604
55 Handschin, C. and Spiegelman, B. M. (2006) Peroxisome proliferator-activated receptor gamma co-activator 1 co-activators, energy homeostasis, and metabolism. Endocr. Rev. **27**, 728–735
56 Seale, P., Bjork, B., Yang, W., Kajimura, S., Chin, S., Kuang, S., Scimè, A., Devarakonda, S., Conroe, H. M., Erdjument-Bromage, H. et al. (2008) PRDM16 controls a brown fat/skeletal muscle switch. Nature **454**, 961–967
57 Longe, H., Romesser, P. B., Rankin, A., Faller, D. V., Eller, M. S., Gilchrest, B. A. and Denis, G. V. (2009) Telomere homolog oligonucleotides induce apoptosis in malignant but not in normal lymphoid cells: mechanism and therapeutic potential. Int. J. Cancer **124**, 473–482
58 Student, A. K., Hsu, R. Y. and Lane, M. D. (1980) Induction of fatty acid synthetase synthesis in differentiating 3T3-L1 pre-adipocytes. J. Biol. Chem. **255**, 4745–4750
59 Ramírez-Zacarías, J. L., Castro-Muñozledo, F. and Kuri-Harcuch, W. (1992) Quantitation of adipose conversion and triglycerides by staining intracytoplasmic lipids with Oil red O. Histochemistry **97**, 493–497

Received 19 June 2009/15 October 2009; accepted 2 November 2009
Published as BJ Immediate Publication 2 November 2009, doi:10.1042/BJ20090928

Biochem. J. (2010) **425**, 71–83 (Printed in Great Britain) doi:10.1042/BJ20090928

online data

SUPPLEMENTARY ONLINE DATA
Brd2 disruption in mice causes severe obesity without Type 2 diabetes

Fangnian WANG*, Hongsheng LIU*, Wanda P. BLANTON*†‡, Anna BELKINA*, Nathan K. LEBRASSEUR§[1] and Gerald V. DENIS*†[2]

*Cancer Research Center, Boston University School of Medicine, Boston, MA 02118, U.S.A., †Immunology Training Program, Boston University School of Medicine, Boston, MA 02118, U.S.A., ‡Section of Gastroenterology, Boston University School of Medicine, Boston, MA 02118, U.S.A., and §Section of Endocrinology, Diabetes and Nutrition, Boston University School of Medicine, Boston, MA 02118, U.S.A.

EXPERIMENTAL

ES cell lines and mice

The RRT234 line of ES cells (BayGenomics) provided the starting point for derivation of homozygous *brd2*$^{(-/-)}$ ES cells by culture in G418. Single colonies were expanded. Both ES cells and mice were genotyped by PCR with a primer set: P1, 5′-GCGTCTGTCTTCCTTGTTTCAG-3′; P2, 5′-CAATCCTCCAGCTCGTCCTAG-3′; and P3, 5′-AAGGTTCATATGGTGCCGTGC-3′. P1+P2 generate a 660 bp wild-type band and P1+P3 generate a 1 kb mutant band. Unless otherwise specified, all primers reported in the present study were homologous to murine genes or transcripts.

Metabolic measurements and IGTT

Mice were housed individually in metabolic cages. We used a comprehensive laboratory animal monitoring system (CLAMS; Columbus Instruments) that was also equipped with photocells to quantify habitual physical activity. For IGTT, 1.5 g of D-glucose/kg of body weight was injected intraperitoneally after starvation overnight. Blood glucose and insulin were measured at the time points described.

Plasmid construction

A Brd2 siRNA expression vector, pSiBrd2, was constructed using pRNA-U6.1/Neo (GenScript), according to the manufacturer's protocol. The sense sequence is 5′-AGATGGGGCAGGAAGGCTCCG-3′. The annealed synthesized double-stranded fragment was cloned into the BamHI and HindIII sites of the vector. pRNA-U6.1/Neo/CTL (GeneScript) was used as a negative control (pSiC) for Brd2 shRNA. To construct pmBrd2, the long-form Brd2 expression vector, mouse Brd2 cDNA was obtained from R1 murine ES cells (American Type Culture Collection) that express a high level of Brd2 by RT–PCR using the primers 5′-GTGGTC GGTACCATGGTGCAAAACGTGACTCCCCACA-3′ and 5′-GGCTAGGAATTCAATCGTATTTTGTCCATG-3′. The cDNA was then ligated into KpnI and EcoRI sites of pcDNA3.1 (+). The pcDNA3.1 empty vector was used as a negative control for Brd2 overexpression.

Immunohistochemistry

Paraffin-embedded sections were deparaffinized and rehydrated, then incubated with rabbit polyclonal antibody against Brd2, as described in main text, and a guinea-pig antibody against insulin (Invitrogen). Alexa Fluor®-conjugated secondary antibodies were Alexa Fluor® 594 anti-rabbit and Alexa Fluor® 488 anti-guinea-pig (Invitrogen). DNA counterstain was with DAPI (4′,6-diamidino-2-phenylindole).

Flow cytometry

BrdU incorporation

β-TC-6 cells in six-well plates were pulsed with 10 μM BrdU for 30 min. Then the cells were fixed and stained using a BrdU Flow Kit (BD Biosciences) with a FITC-conjugated anti-BrdU antibody, and DNA content was determined with 7-aminoactinomycin D. All flow cytometry antibodies were from eBioscience unless otherwise specified.

Macrophages

Primary adipose tissues were isolated immediately after killing of the mice and cells of the SVF were isolated by collagenase-1 digestion (1 mg of enzyme/g of tissue; ICN Biomedicals) at 37 °C for 1 h and centrifugation in the cold. Erythrocytes were removed (1× RBC lysis buffer), then nucleated cells were stained with a FITC-conjugated anti-F4/80 antibody ($IgG_{2a,\kappa}$ clone BM8) in the presence of an F_c-blocking antibody (CD16/32 clone 93). The isotype control was a FITC-conjugated rat $IgG_{2a,\kappa}$ antibody. The HFD (Figures 3E and 4D in the main paper) was D12492 (Research Diets), with 60 % kcal % from fat (where 1 kcal≡1 kJ).

Splenic lymphocytes

Spleens were harvested from 3 month-old *w/lo* female mice or age-matched *w/w* controls and stained with an APC (allophycocyanin)-conjugated anti-B220 antibody as a pan-B-cell marker and a PE (phycoerythrin)-Cy5 conjugated anti-MHC class II antibody in the presence of an F_c-blocking antibody. Lymphocytes were gated by forward- and side-scatter properties, and appropriate isotype controls were used to set the colour gates. Cell cycle parameters and surface markers of stained cells were measured at the BUSM Flow Cytometry Core Facility using an LSR II multi-laser bench top flow cytometer (BD Biosciences). Fluorochrome compensation and population analysis was performed with FlowJo software.

3T3-L1 pre-adipocyte differentiation and insulin resistance

Culture and induction of differentiation of 3T3-L1 cells were as follows: confluent 3T3-L1 pre-adipocytes in 12-well plates were differentiated for 8 days with initiation mixture containing 10 μg/ml insulin, 1 μM dexamethasone and 0.5 mM 3-isobutyl-1-methylxanthine (all from Sigma). Neutral lipid content relative to mock transfection was measured by Oil Red O stain. Induction of insulin resistance with TNF-α and glucose uptake assay were performed as follows: confluent 3T3-L1 pre-adipocytes were differentiated for 10 days with 10 μg/ml insulin, 1 μM dexamethasone, 0.5 mM 3-isobutyl-1-methylxanthine and 1.5 μM pioglitazone (Alexis Biochemicals). Mature adipocytes were treated with 4 ng/ml TNF-α (Cell Sciences) for 4 days to

[1] Present address: Cardiovascular, Metabolic and Endocrine Diseases, Pfizer Global Research and Development, Groton, CT 06340, U.S.A.
[2] To whom correspondence should be addressed (email gdenis@bu.edu).

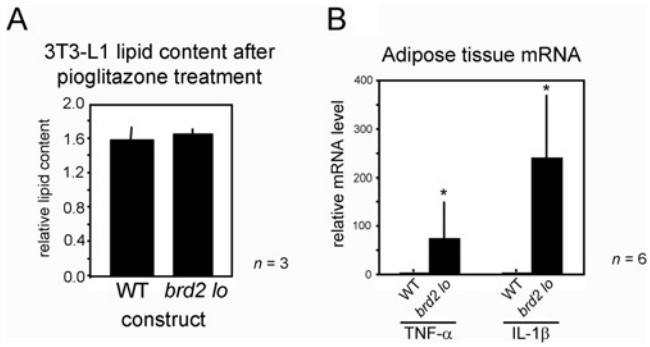

Figure S1 Knockdown of Brd2 affects 3T3-L1 adipogenesis and subsequent insulin sensitivity.

See Figures 4H, 4I, 6B and 6C in the main text. In control experiments, we established that differentiation of 3T3-L1 pre-adipocytes is not blocked by knockdown of Brd2. The enhanced adipogenesis in 3T3-L1 pre-adipocytes observed in the context of Brd2 knockdown was due to increased PPAR-γ activity when no agonist was added to the medium. When a PPAR-γ agonist (pioglitazone) was used, 3T3-L1 pre-adipocytes differentiated to a similar extent, whether Brd2 was knocked down or not, as measured by lipid content (**A**) ($n = 3$). Thus knockdown of Brd2 in 3T3-L1 pre-adipocytes does not interfere with their ability to undergo differentiation. We found that not only were pro-inflammatory cytokines elevated in the serum of obese *w*/*lo* mice at 9 months of age (Table 1 in the main paper), but the mRNA levels of pro-inflammatory cytokines were also elevated in adipose tissue. We assayed *Tnf* (TNF-α) and *Il1b* (IL-1β) transcripts by real-time PCR of visceral fat depots in *w*/*lo* mice and *w*/*w* mice ($n = 6$; $P < 0.05$) (**B**). The transcript level of *Il1b* in WAT (white adipose tissue) from *w*/*lo* mice, for example, was elevated to a mean value of 250-fold in excess of the transcript level in WAT from *w*/*w* mice. These results suggest that WAT contributes at least part to the elevated serum levels of pro-inflammatory cytokines observed in obese *w*/*lo* mice.

Table S1 Numbers of observed compared with expected pups of litters descended from RRT234 chimaeras

Values are the observed numbers (with expected values in parentheses). The expected Mendelian frequency of *w/w*:*w/lo*:*lo/lo* is 1:2:1, supplying two degrees of freedom (ν) for a χ^2 analysis of the observed frequencies. In each case, a significance level (α) of 0.05 was chosen. For 62 neonates, $\chi^2 = 14.52$, and for 108 weaned mice, $\chi^2 = 33.04$, both of which exceed the critical value 5.991 for $\alpha = 0.05$ and $\nu = 2$. Thus Mendelian frequencies were not observed in litters because homozygous mice were highly under-represented among survivors. For 27 E14.5 embryos, $\chi^2 = 1.20$; for 26 E18.5 embryos, $\chi^2 = 4.38$; and for 19 E20.5 embryos, $\chi^2 = 4.26$. Although these embryos are few in number, the sample size is large enough to calculate an unbiased χ^2. The ratios for embryos are Mendelian, leading us to speculate that some homozygous embryos are capable of surviving until birth, but the pups are generally not viable. This interpretation is consistent with the results by Gyuris et al. [34], who report that lethality increased towards the end of embryonic development of homozygous mice derived from RRE050 ES cells (25 out of 28 homozygous embryos died before birth), which is more severe than the phenotype reported in the present study for homozygous mice derived from RRT234 ES cells.

	Age				
Litter	E14.5	E18.5	E20.5	Neonate	Weaned (3 weeks)
Total	27	26	19	62	108
w/w	9 (6.75)*	7 (6.5)	5 (4.75)	23 (15.5)	32 (27)
w/lo	13 (13)	17 (13)	13 (9.5)	36 (31)	76 (54)
lo/lo	5 (6.75)	2 (6.5)	1 (4.75)	3 (15.5)	2 (27)
χ^2	1.20	4.38	4.26	14.52	33.04

induce insulin resistance. For the glucose uptake assay, cells in 12-well plates were treated with or without 170 nM insulin for 30 min at 37 °C, then with 1 μCi/ml [^{3}H]-2DG (2-deoxyglucose) for 5 min. Uptake of [^{3}H]-2DG was determined with a scintillation counter.

Real-time PCR

Total RNA from cultured cells or tissues was extracted with TRIzol® (Invitrogen) and cDNA was prepared with the ImProm-II reverse transcription system (Promega). Real-time PCR was performed using SYBRGreen PCR master mix (Applied Biosystems). Relative mRNA levels were determined by $\Delta\Delta Ct = \Delta C_{t,\ sample} - \Delta C_{t,\ reference}$ and β-actin was the reference. Real-time PCR primers for assay of transcripts from pro-inflammatory cytokine genes were as follows (F, forward; R, reverse). For *Tnf*: F, 5′-CTCCAGGCGGTGCCTATG-3′ and R, 5′-GGGCCATAGAACTGATGAGAGG-3′; and for *Il1b*: F, 5′-GCACACCCACCTGCA-3′ and R, 5′-ACCGCTTTTCCATC-TTCTTCTT-3′. Other primers were as follows. For *Ins* (insulin): F, 5′-GGGGAGCGTGGCTTCTTCTA-3′ and R, 5′-GGG-GACAGAATTCAGTGGCA-3′; for *Brd2*: F, 5′-TACTGGG-CTGCCTCAGAATG-3′ and R, 5′-CCAGTGTCTGTGCCAT-TAGGA-3′; and for *Actb* (β-actin): F, 5′-CCCAGATCATGTTT-GAGACCTTC-3′ and R, 5′-AGTCCATCACAATGCCTGT-GGTA-3′. Primers for assay of transcripts from Ucp genes were as follows. For *Ucp1*: F, 5′-CCCGACAACTTCCGAAGTGCA-3′ and R, 5′-GGAAGCCTGGCCTTCACCTTG-3′; and *Ucp2*: F, 5′-CTACAAGACCATTGCACGAGAGGA-3′; and R, 5′-GA-GGTTGGCTTTCAGGAGAGTATC-3′; for *Ucp3*: F, 5′-CATC-GCCAGGGAGGAAGGAG-3′ and R, 5′-TCCAAAGGCA-GAGACAAAGTGAC-3′; and for control transcripts, *Tbp*: F, 5′-ACCCTTCACCAATGACTCCTATG-3′ and R, 5′-TGACTGCAGCAAATCGCTTGG-3′.

Protein immunoblot and co-immunoprecipitation

For co-immunoprecipitation, antibodies were cross-linked to Protein A/G beads using dimethylpimelimidate, according to the manufacturer's instructions (Pierce). The cross-linked antibodies were washed extensively before binding to cell lysates. Reagents used were rabbit polyclonal Brd2 antibody [14], monoclonal and polyclonal PPAR antibodies and Protein A/G Plus agarose (Santa Cruz Biotechnology), monoclonal GAPDH (glyceraldehyde-3-phosphate dehydrogenase) antibody (Millipore) and β-actin polyclonal antibody (Sigma).

Statistical analysis

Histological images in Figures 2 and 5 of the main paper were analysed with NIH Image J software, version 1.41o. Adipocyte area was calculated from best polygon fit to individual adipocytes measured in three separate fields for each genotype and each tissue type. The area distribution for wild-type adipocytes was calculated in SigmaPlot 11.0 using non-linear regression to a five parameter Weibull curve. Pancreatic β-cells were counted in Image J by converting RGB micrographs into eight-bit greyscale, then defining a threshold value such that each stained nucleus was counted once using the 'analyse particles' function; the number of nuclei were then taken as a proxy for the number of β-cells, which was expressed as a box plot. The boundary of the box closest to zero indicates the 25th percentile, a line within the box indicates the median and the boundary of the box farthest from zero indicates the 75th percentile. Error bars indicate the 90 and 10th percentiles, and outliers were identified. Islet area was calculated as for adipocytes. Linear regression and statistical tests for significance were performed in SigmaStat 3.11.

Received 19 June 2009/15 October 2009; accepted 2 November 2009
Published as BJ Immediate Publication 2 November 2009, doi:10.1042/BJ20090928